248500-1-F

Final Report

EXAMINATION OF THE PHYSICAL, ELECTRICAL, AND MICROWAVE EVOLUTION OF WATER INTO YOUNG SEA ICE

Robert G. Onstott

Center for Earth Sciences
Advanced Concepts Division

May 1993

Office of Naval Research
Department of the Navy
800 N. Quincy Street
Arlington, VA 22217-5000
Scientific Officer: Charles A. Luther
Contract No.: N00014-92-C-0140

ERIM
Ann Arbor, MI 48113-4001

REPORT DOCUMENTATION PAGE

Form Approved
OMB No. 0704-0188

1. AGENCY USE ONLY (Leave blank)	2. REPORT DATE	3. REPORT TYPE AND DATES COVERED
	November 1993	Final 1 Sept. 92 - 28 Feb. 93

4. TITLE AND SUBTITLE
Examination of the Physical, Electrical, and Microwave Evolution of Water Into Young Sea Ice

5. FUNDING NUMBERS
N00014-92-C-0140

6. AUTHOR(S)
R.G. Onstott

7. PERFORMING ORGANIZATION NAME(S) AND ADDRESS(ES)
Environmental Research Institute of Michigan (ERIM)
P.O. Box 134001
Ann Arbor, MI 48113-4001

8. PERFORMING ORGANIZATION REPORT NUMBER
Final 248500-1-F

9. SPONSORING/MONITORING AGENCY NAME(S) AND ADDRESS(ES)
Office of Naval Research
800 N. Quincy Street
Arlington, VA 22217-5000

10. SPONSORING/MONITORING AGENCY REPORT NUMBER

11. SUPPLEMENTARY NOTES

12a. DISTRIBUTION/AVAILABILITY STATEMENT
Unlimited

12b. DISTRIBUTION CODE

13. ABSTRACT (Maximum 200 words)
Knowledge of the interrelationships between ice thickness, its temperature profile, the distribution of salinity, the dielectric property profile, and the roughness of the air-ice interface is important to the understanding of the backscatter response of new and young sea ice. Backscatter, physical, and electrical property measurements were made during the first 120 hours of growth for a saline ice sheet grown in a laboratory outdoor tank. The purpose of this work is to describe the evolution of open water to ice 15 cm thick. Ambient air temperatures were -15°C. During the critical growth period to 10 cm and then warmed to -10°C during the final 5 cm of growth. Radar backscatter data were obtained at 5.3, 9.6, 13.6, and 16.6 GHz to correlate with the changes in the microwave signatures with ice thickness, ice surface temperature, the salinity profile, the dielectric profile, and modifications which occur naturally to the air-ice interface of the ice sheet. Linear antenna transmit-receive polarizations were used and include vertical-vertical and horizontal-horizontal. Angle of incidence scans were made from vertical to 50°. The change in the backscatter response with changing ice thickness is documented and discussed in terms of the physical-chemical-electrical property changes.

14. SUBJECT TERMS	15. NUMBER OF PAGES
	55
	16. PRICE CODE

17. SECURITY CLASSIFICATION OF REPORT	18. SECURITY CLASSIFICATION OF THIS PAGE	19. SECURITY CLASSIFICATION OF ABSTRACT	20. LIMITATION OF ABSTRACT
Unclassified	Unclassified	Unclassified	Unlimited

ACKNOWLEDGEMENTS

We would like to acknowledge the assistance received by the personnel at USA Cold Regions and Research Engineering Laboratory, especialiy that of Tony Gow and Don Perovich. They have contributed to both the logistics of the work at CRREL and the support in the characterization of the physical-chemical properties of the saline ice sheets.

CONTENTS

FIGURES

FIGURES (CONCLUDED)

TABLES

1.0 INTRODUCTION

To obtain a complete characterization of air-ice-ocean processes which occur in polar regions, the ability to discriminate ice from water, to determine the distribution of ice thickness, and to retrieve physical property information for the ice sheet observed are required. The most viable approach in accomplishing this goal is through microwave remote sensing which does not require operation in sunlight or cloud free conditions. The success of remote sensing techniques improves greatly when based on a thorough understanding of the relationships between sea ice properties and its microwave behavior. In the work described in this report, a study was conducted to isolate and identify individual physical-chemical-electrical property changes and the resultant change in backscatter behavior. A saline ice sheet was grown which was horizontally homogeneous. Its thermal history and physical characteristics were closely monitored and documented. This study of the evolution in the microwave and physical properties of first year ice began with the freezing of a large pool of sea water. At the end of 120 hours the ice sheet obtained a thickness of 15 cm. Key issues evolve concerning the knowledge of the interrelationships between ice thickness, the ice temperature profile, the distribution of salinity within the ice sheet, the dielectric property profile, the roughness of the air-ice interface, and the backscatter response. These experiments were conducted at a facility of the U.S. Army Cold Regions Research and Engineering Laboratory (CRREL) located in New Hampshire and during the coldest portion of the winter season (January). The goal of improving the understanding of the relationship between ice properties and their microwave response is important for the improvement in the ability to convert the microwave signal information into useful and accurate geophysical data products. Previous studies of the radar-ice interaction process indicate that the most critical influences to the backscatter process are ice surface roughness, the permittivity of the

ice sheet, and, for multiyear ice, the size of the air bubbles in the upper most layers. In addition, the presence of a snow layer may have a range of impacts, some significant and some not (Carsey et al., 1992).

This experiment was devised as a means to simplify experimentation, to allow a more complete collection of a wide range of possible sensor parameters, to allow for some control in the physical and chemical properties of the ice sheet in a way not possible in a field investigation, and to provide an opportunity to be as meticulous as necessary in producing a description of the ice physical properties.

Active microwave observations of the saline ice were made under quiescent conditions, only wind induced ripples were present. The radar backscatter measurements were made at 5.3, 9.6, 13.6, and 16.6 GHz. Antenna transmit-receive polarizations included vertical-vertical (VV) and horizontal-horizonal (HH), and angles of incidence ranged from vertical to 50°. During this investigation the structure and salinity profiles of the ice sheet, the thickness and surface temperature, surface roughness and dielectric properties were examined.

1.1 DESCRIPTION OF THE MEASUREMENT FACILITY

A sheet of sea ice was grown during winter (January) to closely simulate Arctic sea ice grown under quiescent conditions. Crystalline texture and salinity profiles of the ice were made and compared with those obtained of ice in the Arctic to gauge success. The simulation was judged successful. The ice sheet measured 5 x 12 m and floated on about 1.5 m of sea water. A detailed description of the facility and ice growing procedure is described in a paper by Arcone, Gow and McGrew (1986). An industrial gantry was used to position the microwave instrumentation at a 3 m height above the ice sheet. Along- and across-track positions were varied by moving the gantry up and down rails which were positioned along the side of the ice tank and by positioning the antenna cluster about the gantry I-beam. An antenna-gantry

structure allowed the electro-mechanical rotation of the antenna-RF assembly. This permitted the observation of the microwave behavior at various incidence angles and to measure the scatterometer noise floors by pointing at an unobscured sky.

1.2 DESCRIPTION OF THE RADAR SCATTEROMETER AND MEASUREMENT PROCEDURE

The radar scattering behavior was described using a calibrated frequency-modulated continuous-wave scatterometer. A parabolic dish antenna equipped with a dual-ridged waveguide feed was used in combination with two standard gain horns operating at 8-12 and 12-18 GHz. Two additional standard gain horns were used for operation at 4-8 GHz. Footprint sizes at 40° ranged from 0.1-1.7 m. Each of the antennas were able to be rotated 90° to change polarizations from vertical (V) to horizontal (H). Specifications of the radar scatterometer are summarized in Table 1. The scatterometer was translated in both the along- and across-track directions to obtain multiple spatial samples to improve the estimate of the mean radar scattering coefficient. Absolute calibration was performed by measuring the backscatter power from a Luneberg lens reflector with known radar cross sections for each of the radar frequencies. Instantaneous calibration was performed using signal injection to take into account short-term fluctuations in transmitter power. The system noise floor was documented periodically by recording the power return when the radar was pointed at the sky. Major ice forms investigated included calm water, grease ice, dark nilas, and grey ice. Ice had grown to a thicknesses of 14.5 cm.

Table 1.
Radar Scatterometer System Specifications

PARAMETERS	FREQUENCY - GHz			
	5.3	9.6	13.6	16.6
Type	FM-CW			
FM Sweep	1.9 GHz			
Intermediate Frequency	15 kHz			
IF Bandwidth	3.5 kHz			
Antenna Two-Way Beamwidths	18°	6.7°	6.1°	4.7°
Height	2.7 m			
Incidence Angle Range	Vertical to 50°			
Calibration	Short Term - Delay Line Absolute - Luneberg Lens			

2.0 ICE SHEET CHARACTERISTICS

For a comprehensive review of the growth, structure and properties of sea ice the interested reader is referred to Weeks and Ackley (1982). An ice sheet is composed mainly of vertically columnar crystals. The growth of vertically columnar crystals may be initiated almost immediately by using a nucleation process as discussed by Gow (1986). How quickly the ice transforms from a random crystal structure to the vertically columnar structure is influenced during the initial growth stage by the turbulence in the water column and the number of small particles which are deposited at the air-water interface. Saline ice produced in this manner is indistinguishable from ice observed in the Arctic when grown under calm conditions (e.g. when winds are low and there are no wave modulation effects). When sea water freezes, pure ice and brine are produced. Active and passive microwave sensors sense the electrical characteristics of the ice sheet. Hence, the brine inclusions, located between the long vertical ice crystal plates, influence greatly the microwave response. The size, volume and concentration of brine in these inclusions are sensitive to a number of factors, but mainly the temperature at its location. The volume of brine in the ice sheet directly impacts its permittivity and influences its ability to scatter and transmit energy.

2.1 DESCRIPTION OF THE ICE FORMATION DURING THE EXPERIMENT PERIOD

The ice sheet was grown in calm sea water with a salinity of 22 ppt. Interior ice salinities ranged from 16 parts-per-thousand (ppt) when very new (0.8 cm) to 5.5 ppt after 120 hours (an ice thickness of about 15 cm). The ice sheet gave the visual impression of being spatially homogenous. This was confirmed later with the radar through a series of observations which were closely spaced across the width of the ice sheet. The ice sheet surface was very smooth throughout the duration of the observations series. Root mean square vertical heights and correlations lengths of

0.05 cm rms and 1-2 cm, respectively, were typical.

An ice thickness was measured for each set of radar measurements. Surface temperatures were measured periodically with a calibrated mercury thermometer placed in contact with the ice surface and covered with an insulating foam. Salinity measurements were made of immediately prepared samples extracted from the ice sheet with a Beckman solubridge which has an estimated accuracy of ± 0.2 ppt. Ice sheet texture analyses were performed using thin ice sections made with a microtome. Details of these observations and techniques are described in Arcone, Gow and McGrew (1986) and Weeks and Gow (1979). Ice sheet surface roughness measurements were made of ice extracted from the ice sheet. Thick sections were machined and then photographed against a calibrated grid. Photos were mosaicked and digitized, and then statistics of rms height and correlation lengths were calculated.

2.2 PHYSICAL AND ELECTROMAGNETIC MODEL FOR YOUNG FIRST-YEAR SEA ICE

In Figure 1, a physical model for sea ice is presented to describe the important interfaces and regions for scattering for very-young sea-ice observed in this study. Five dielectric layers and three interfaces are of particular interest. The ice sheet is sandwiched between air and sea water. The interface which adjoins the atmosphere begins as an air-water interface and makes two cycles from air-brine to air-ice. A brine layer is present during the earliest stage of sea ice growth, when there is a rapid expulsion of brine to the surface in association with cooling of the upper ice sheet (e.g. occurs at about 2 cm) or when solar radiation promotes its production. If ambient conditions warm, excess brine may migrate to the surface. When ice becomes thick and cold this layer may no longer be present. The thickness of a brine layer is not well described, but our visual estimates suggest that it is less than 0.25 mm, typically. A radar may be used to propagate an electromagnetic wave to an ice sheet. Energy is reflected, scattered, and transmitted due to interaction with the air-

CES-92-105-1

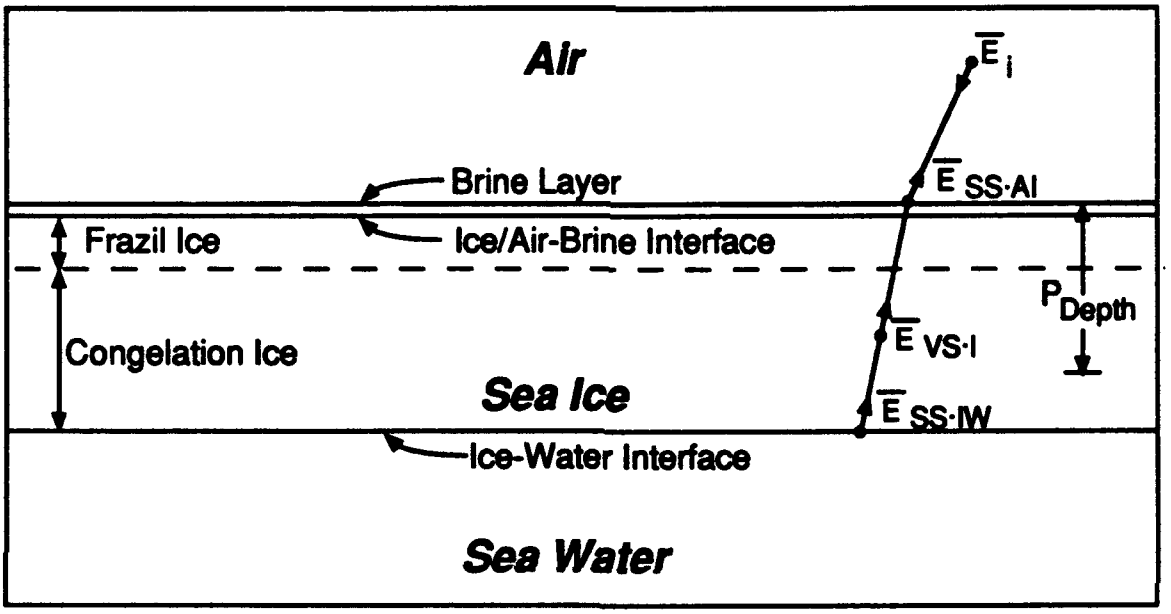

Figure 1. Physical and Electromagnetic Model for New and Young Sea Ice Is Composed of a Brine Surface Layer, a Thin Frazil Layer, and Congelation Ice. The Incident Electric Field Scatters Back to the Radar Due to a Rough Air-Ice Interface, Scattering From Within the Ice Volume, and Scattering Related to the Ice-Water Interface (When the Ice Is Thin). The Penetration Depth P_{depth} Represents the Distance That a Radiowave Propagates and Whose Backscatter Intensity Is Reduced to e^{-1}.

ice interface. Propagation into the ice sheet may result in additional scattering or reflection at the ice-water interface. The components of the scattered field which originate at the air-ice sheet interface ($E_{ss.ai}$), from the volume within the ice sheet ($E_{vs.i}$), or from the ice-water interface ($E_{ss.iw}$) are identified in Figure 1.

The depth at which the intensity of the radio wave reduces to a value of e^{-1} is denoted as the penetration depth. This depth is important in that it may be shown that the layer corresponding to one penetration depth often dominates the scattering process. However, for a complete characterization of the scattering process, 2-3 layers may be needed. As an example, if the penetration depth resides within the ice sheet, it is unlikely that the reflection from the ice-water interface contribution is important. For the cases where the penetration depth is greater than the ice thickness, this interface must be accounted for, either by adding the $E_{ss.iw}$ component to the scattering process or by inclusion in the calculation of the total reflectivity of the ice sheet as presented to the radar.

When an ice sheet grows under calm conditions the ice sheet is found to have a naturally smooth ice-air interface (surface heights of 0.05 cm rms were measured). The bottom interface also mimics the tops surface (surface height of 0.05 cm rms) for new and thin ice. The ice sheet is largely composed of ice with long vertical crystals and is called congelation ice. However, a thin layer of randomly oriented crystals which are small in size is present at the air-ice interface. This layer is called the frazil ice layer. For our observations this layer is less than 5 mm thick. If ripple or wave conditions during early ice formation are more dynamic, this layer will be thicker. The salinity of an ice sheet (> 22 ppt) will be less than that of the sea water (i.e. 22 ppt in this case) from which it is born. The brine layer may, however, attain values greater than 130 ppt.

A backscatter response may be dominated by pure surface scattering, pure volume scattering, or their combination. If the dominant scattering mechanism is due

to the surface, the scattering coefficient σ° may be described as

$$\sigma^\circ_{pp}(\theta_{inc}) = K\,\Gamma^2(pp, f, \theta_{inc}, \epsilon_r^*)\,SF(pp, f, \sigma_{surf}, l_{surf}) \quad (1)$$

where *pp* is the polarization, K is a scaling constant, Γ is the reflection coefficient, f is the radar frequency, θ_{inc} is the incidence angle, ϵ_r^* is the complex dielectric constant, SF is a function which describes the shape of the angular response, σ_{surf} is the surface height rms, and l_{surf} is the surface height correlation function. The expression is written in this simplified form to illustrate that there are two critical parameters which influence backscatter in the cases encountered in our observations. They are the complex dielectric constant ϵ_r^* which sets the absolute backscatter level through the reflection coefficient, the surface roughness statistics σ_{surf}, and l_{surf} which also contributes in determining the absolute level and the angular response of the backscatter. When the roughness statistics are held constant as they were in this study, the rise and fall in the backscatter response may be associated with the change in dielectric constant profile or the presence of a brine layer.

Scattering from within a volume arises due to discontinuities in the dielectric properties in the volume. This may be associated with changes in either electrical or physical properties. An ice sheet is composed of pure ice, brine, and gas, each of which have dissimilar electrical properties. Brine contained in pockets, channels, or tubes, and gas bubbles are the key sources of dielectric continuity. Each contribute to the production of volume scattering. A zeroth-order expression of volume scattering may be written as

$$\sigma^\circ_{pp}(\theta_{inc}) = \sigma^\circ_s(\theta_{inc}) + T^2(\theta_{inc})\,\sigma^\circ_v(\theta'_{inc}) \quad (2)$$

$$\sigma^{\circ}_{v}(\theta_{inc}) = N\sigma_{b}\cos(\theta'_{inc})\,(1-L^{-2}(\theta'_{inc}))\,/\,(2k_{e}) \qquad (3)$$

$$\sigma_{b} = 4\pi r^{6}\epsilon_{b}'^{2}k_{o}^{4}\Gamma_{AI}^{2} \qquad (4)$$

where σ°_{pp} is the total backscatter, θ_{inc} is the incidence angle, σ°_{s} is the contribution from surface scattering, T^2 is the effect of transmission through the air-ice interface, σ°_{v} is the volume scatter contribution from the ice interior, θ_{inc}' is the incidence angle in the ice interior, N is the total number of discrete scatterers and equal to $f_{vf}/(4\pi r^3/3)$, f_{vf} is the volume fraction and equal to $(1 - \rho/0.926)$, ρ is the density of the ice, σ_b is the radar cross section of an individual bubble, L^2 is the attenuation loss associated with propagation through the scattering layer, k_e is the extinction coefficient, r is the radius of the bubbles, ϵ_b' is the dielectric constant of the sea ice, k_o is the wave number, and Γ is the Fresnel reflection coefficient (Kim et al. 1984ab and Kim, 1984). The above expressions are used to demonstrate how volume scattering from discrete particles is proportional both to the radii cubed when the particle is a sphere, and to the density and thickness of the layer, so that the total number of scatterers may be taken into account. Also note that the relationship between the wavelength of the radar and the size of the particle is important if the backscatter produced is to be of significance. A diagram is provided in Figure 2 to shown the geometry associated with surface and volume scattering.

A diagram is provided in Figure 3 to illustrate how the backscatter response of sea ice may change according to scattering from a very-smooth surface, a moderately rough surface, a rough surface, and an ice sheet, which produces a strong volume scattering. Key features illustrated are that for smooth surfaces backscatter is strongest closest to vertical incidence and that as the ice sheet becomes rougher, the vertical incidence component reduces and energy at the larger angles increases. The

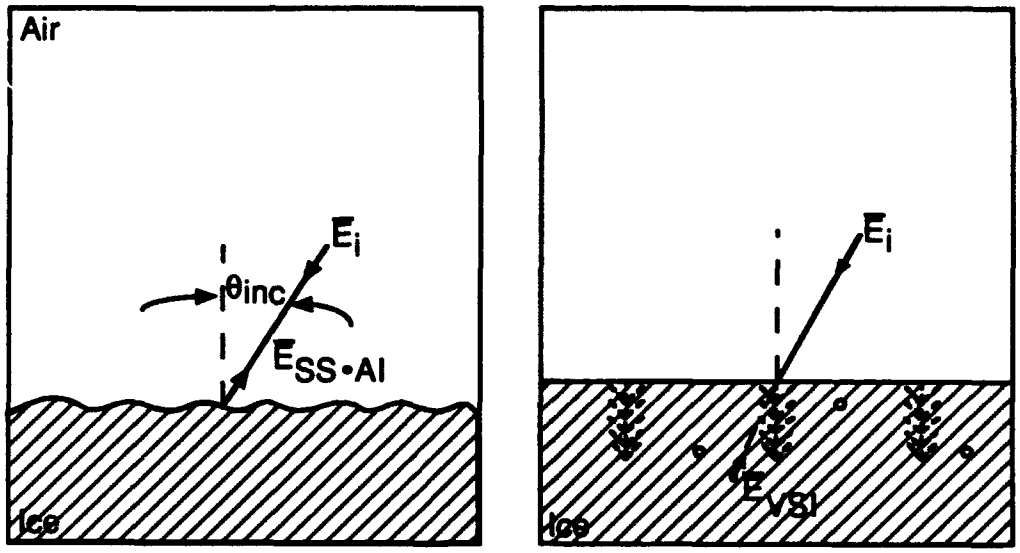

Figure 2. The Backscatter From Sea Ice May Arise Due to Scattering From the Surface, the Interior of the Ice Sheet, and the Combination of These Two Mechanisms. In (a) the Scattering From a Rough Surface Is Indicated. In (b) the Volume of the Ice Sheet is Illustrated to Show That for First Year Ice the Distribution of Brine Pockets and Channels May Be a Source of Volume Scattering.

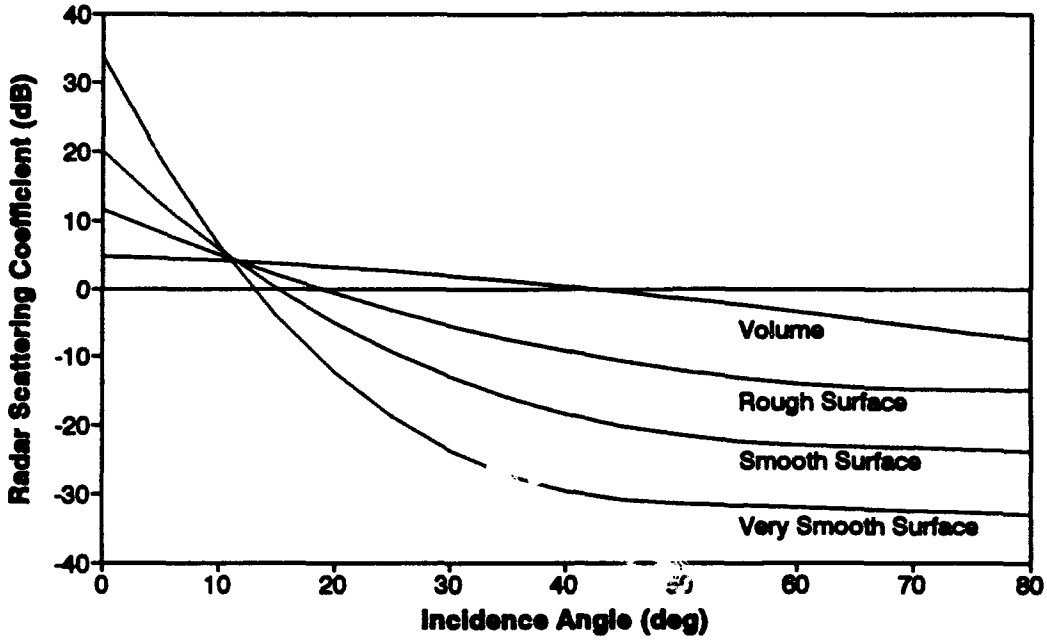

Figure 3. The Backscatter Response for a Set of Idealized Smooth and Rough Surfaces and Volume Scattering Is Shown as a Family of Curves to Present the General Characteristics of Each Response.

key characteristic of volume scattering is an angular response that is slowly decaying and is enhanced at the large angles. Scenes which produce backscatter from both surface and volume scattering may appear as the superposition of the two scattering responses described above.

3.0 ACTIVE MICROWAVE OBSERVATIONS

Knowledge of the interrelationships between ice thickness, its temperature profile, the distribution of brine volume, the dielectric property profile, and roughness of the air-ice interface is important to the understanding of the backscatter response of new and young sea ice. Measurements have been made by Onstott (1991, 1985) and others to examine the time series response of newly formed sea ice. A summary of physical property observations during this investigation is presented in Figure 4 and Table 2. In this report, data associations will be referred to by the thickness of the ice sheet. "Line" plots are used to allow for a presentation which is easy to interpret and examine, otherwise a majority of the measurement data for the thinnest cases would be compressed at the origin. Observation number, growth interval, ice sheet thickness (δ_{ice}), air temperature (T_{air}), ice surface temperature (T_{ice}), and bulk salinity (S) are summarized in Table 2.

3.1 REFLECTIVITY RESPONSE AT 5.3 GHZ

The time-series response observed at 5.3 GHz is provided in Figure 5 and shows the evolution of open water to grey ice (δ_{ice} = 14.5 cm thick). This response is shown at incidence angles of 0°, 25° and 40°, and VV- and HH-polarizations.

State 1: High Dielectric Ice Layer

During the first 31 hour period the ice grew from 0^{+}-9 cm. The air temperature ranged from -13.5° to -15°C. These observations were made at night, hence no solar influence. The response for open water is presented for two conditions, calm water (0-C) and calm water with small ripples present (0-R). There is about a 1 dB difference at vertical incidence and a couple of dB at angles off-vertical.

The reflectivity as observed by the incidence angle response at 0° is reasonably

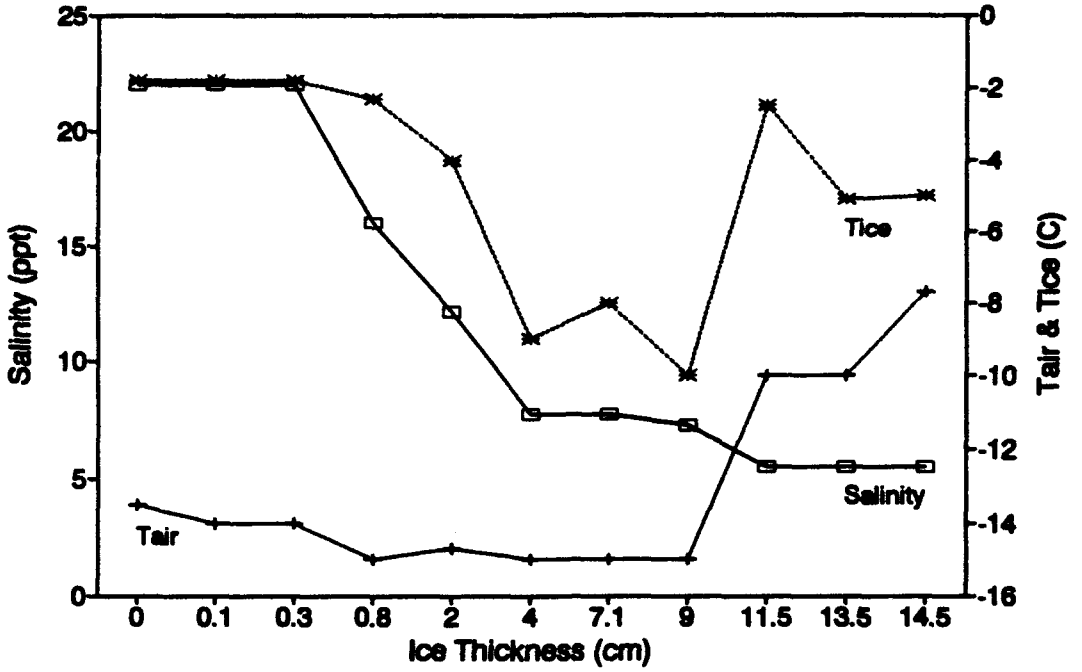

Figure 4. Observations of Air Temperature, Ice Temperature and Bulk Salinity During the Evolution of Water to Grey Ice Are Presented as a Function of Ice Thickness.

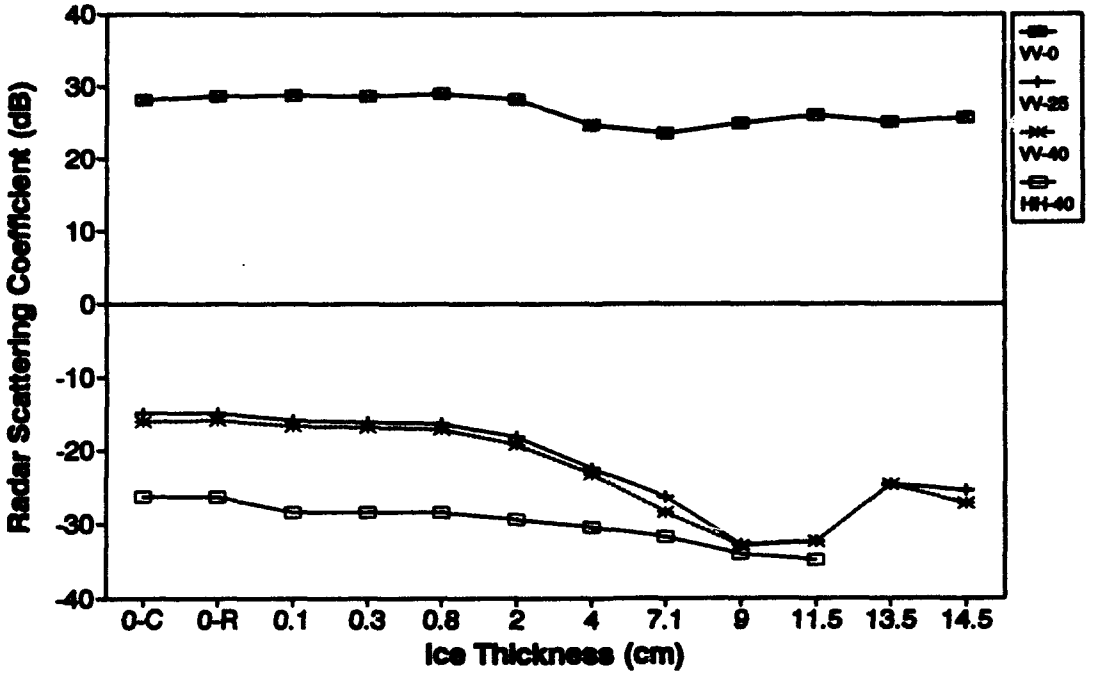

Figure 5. The Time Series Response of the Backscatter at 5.3 GHz Is Shown for the Evolution of Water to Young Ice at Incidence Angles of 0°, 25° and 40° for VV and HH Antenna Transmit-Receiver Polarizations.

Table 2.
Growth Interval, Ice Sheet Properties and Thickness Are Shown for the Experiment Series.

OBS #	GROWTH INTERVAL - hours -	ICE SHEET THICKNESS - cm -	T_{air} - °C -	T_{ice} - °C -	BULK SALINITY - ppt -	COMMENTS
1	0	0	-13.5	-1.6	22.0	Night
2	1.3	0.1	-13.5	-1.6	22.0	Night
3	2.0	0.3	-14.0	-1.6	22.0	Night
4	3.5	0.8	-14.0	-2.3	16.0	Night
5	6.5	2.0	-15.0	-4.0	12.1	Night
6	17.5	4.0	-14.7	-9.0	7.7	Blown Snow Crystals on Natural Surface
7	26.3	7.1	-15.0	-8.0	7.7	δ_{snow} = 1 cm
8	31.0	9.0	-15.0	-10.0	7.3	Smooth and Bare
9	70.0	11.0	-10.0	-6.1	5.5	Sunny and Bare
10	91.0	13.5	-10.0	-5.1	5.5	Morning and No Sun
11	116.3	14.5	-7.7	-5.0	5.5	Sunny Day, But No Sun on Ice

constant (slope of 0.05 with mean square error of 0.4 dB) between the ice thickness range of 0-2 cm. The magnitude of the complex dielectric constant $|\epsilon_r^*|$ was calculated based on reflectivity and $\sigma°(0°)$, and is determined to be 42 ± 9. The dielectric constant for this period may be expected to be similar to that of sea water, since the ice layer is thin compared to the radar wavelength (λ = 5.66 cm) and due to the presence of brine on the ice surface. For sea water at -1.8°C, 22 ppt, and 5.3 GHz ϵ_r^* = 61-j40. At a frequency of 5.3 GHz, the reflectivity is not sensitive to the surface roughness scales observed in this study. Ice of this age is very smooth visually and when compared to the radar wavelengths which range from 1.7-30 cm. A surface is considered smooth by the Fraunhofer criteria when the rms roughness $\sigma_{surface}$ is less than 1/32 of the wavelength when viewing normal to the surface (e.g. at 5.3 GHz the ratio is 1/120th of a wavelength).

During the first 31 hour period with near constant air temperature (-15°C), the sea water froze and a horizontally homogeneous ice sheet grew in thickness from 0^+-9 cm, and the ice surface cooled, reducing in temperature from -1.6° to -4°C. The reflectivity (at 5.3 GHz), however, changes little. It stays within 7% of the mean. However, as is best noted in the slope of the radar scattering coefficient $\sigma°$ response at 25° or 40°, there is a significant decrease in the radar scattering coefficient at the middle angles. The mechanism for this decay is noted in the visual observations presented in Figure 6 and is discussed in the section which follows.

State 2: Low Dielectric Ice Sheet

Once freezing is initiated under calm conditions, an ice skim forms on the sea water and then quickly evolves into a complex of stellar ice crystals as shown in the photograph in Figure 6a. By 2 cm, it is observed that a major transition is underway and that the backscatter response at $\sigma°_{vv}(40°)$ is reducing much faster than at normal incidence. This indicates that, at a minimum, two processes are at play. The nadir

(a)

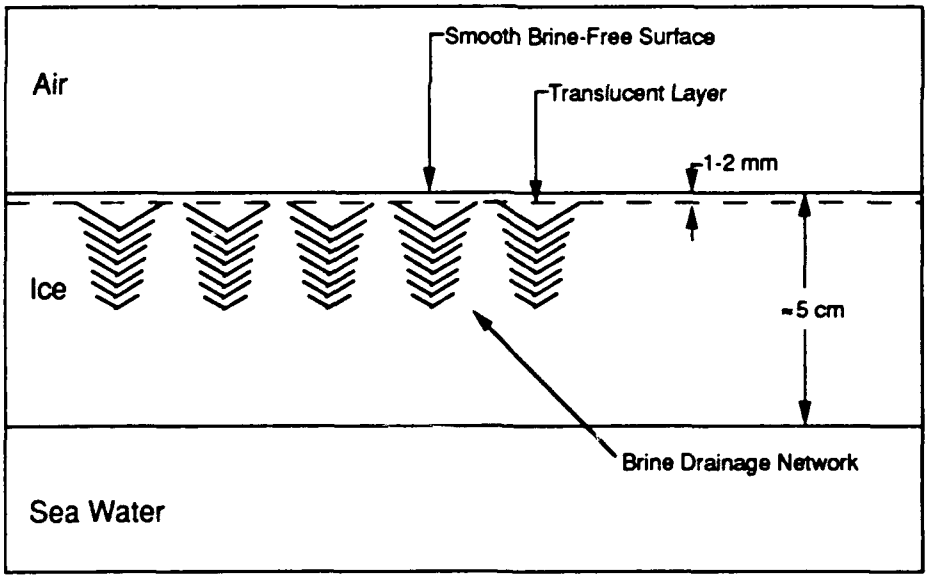

(b)

Figure 6. In (a) a Photograph Shows the Ice Surface and Stellar Ice Crystals for Ice at 1 cm Thickness, in (b) a Cartoon Details the Vertical Construction of New Ice Once It Has Attained a Low Dielectric Constant. It Is Characterized by a Smooth Ice-Air Interface, a Thin Bubble-Free Layer (1-2 mm Thick), and an Interior Brine Distribution Network.

response responds directly to the change in total reflectivity. Total reflectivity is controlled by the dielectric constant profile, the thickness on the ice sheet, and the dielectric constant of the sea water layer. The response at 40° is sensitive to both the change in dielectric constant and changes in surface roughness statistics. The ice surface appears to become smoother beginning at an ice thickness of about 1 cm and continues to about 5 cm.

The characteristics of the second state is shown in Figure 6(b). The air-ice interface is now even smoother, a layer of fresh water origin with a thickness between 1-2 mm (attributed to the seeding process of adding freshwater to initiate the growth of congelation ice) is present immediately below the ice-air interface, and is then followed by a saline layer with prominent upside-down tree-like brine organizations.

The metamorphosism observed is gradual during the first 6.5 hours and culminates into a state change by 20 hours of growth and 4 cm thick ice. Based on the measurement of radar reflectivity at vertical, the magnitude of the dielectric constant $|\epsilon_r^*|$ after the state change is about 7. The full dielectric response is shown in Figure 7. The surface roughness was determined to be 0.05 cm rms and the ice surface temperature had cooled to -4°C. By accounting for the change in the dielectric constant between these two states, the roughness for the initial ice layer is estimated to be 0.065 cm rms. This estimate is based on predictions made utilizing the small perturbation model (Ulaby et al., 1982) which is applicable for a dielectric surface which is very smooth compared to the radar wavelength.

A null in the time series of the backscatter response occurs at an ice thickness of about 7 cm, 6 hours after transitioning from State 1. The change in the magnitude of the dielectric constant is from 44 (δ_{ice} = 0.1 cm) to 5.5 (δ_{ice} = 7 cm). In summary, these observations document a transition from an ice-water layer composite with a high dielectric constant (State 1) to an ice layer (and electromagnetic half-space) which presents a low dielectric constant (State 2) to the

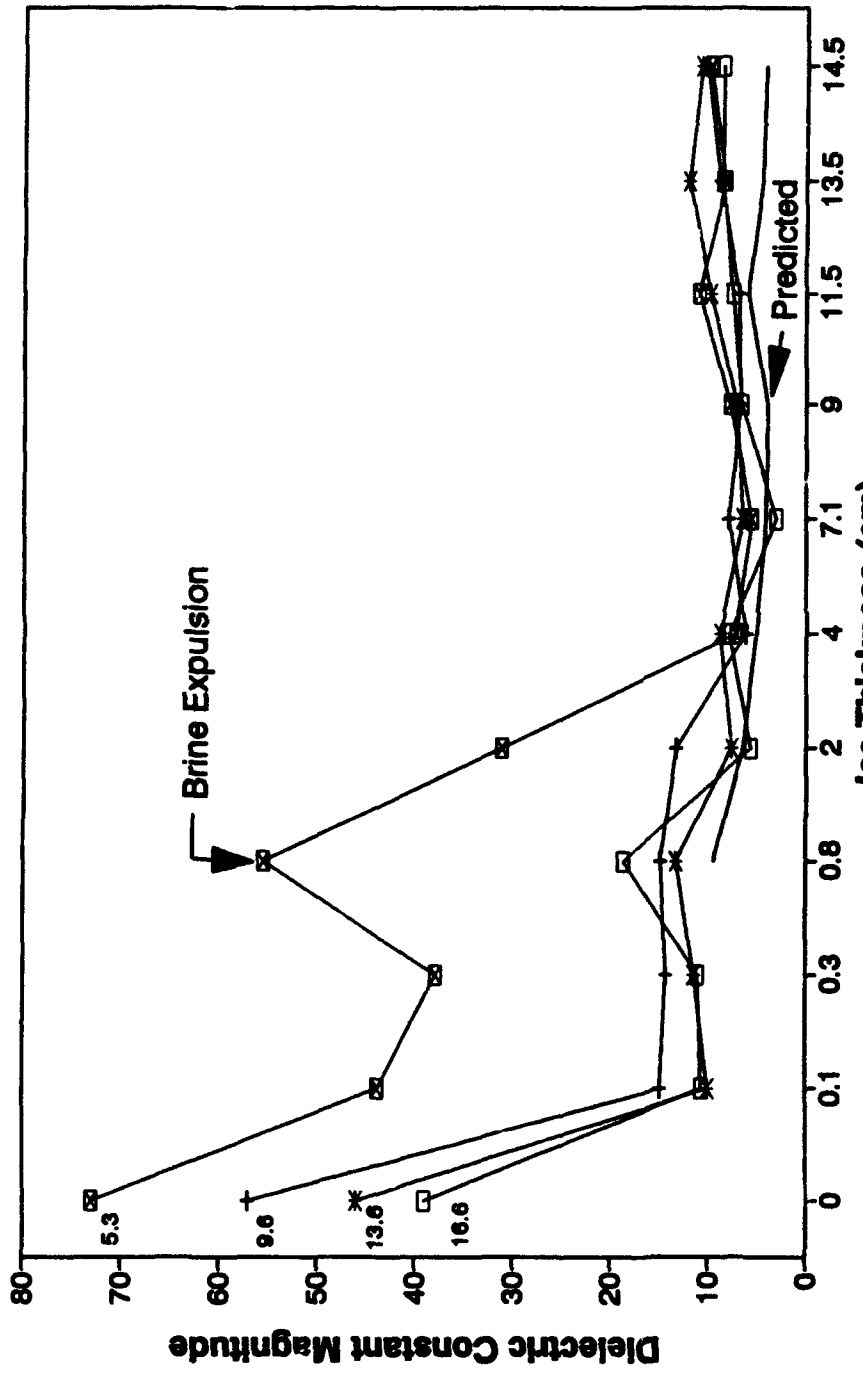

Figure 7. The Magnitude of the Complex Dielectric Constant $|\epsilon_r^*|$ Is Derived From the Measurement of Reflectivity and Is Shown For 5.3, 9.6, 13.6 and 16.6 GHz. The Values Predicted Based on a Mixing Model for the Observed Ice Conditions Are Also Included.

radar, and that occurs within 1 day of the initiation of ice formation. As will be shown later, this transformation takes place quickly at the higher frequency.

State 3: Effect of Solar Heating

Later in the observation period, ice sheet temperatures increased due to daytime solar heating coupled with ambient air temperatures reaching -10°C. Upper ice sheet dielectric properties (magnitude) are found to increase to values of 8 to 11. The doubling in the reflectivity and measured dielectric constant illustrates clearly the importance of upper ice sheet temperatures, the accompanying dielectric constant response, and importance of free water or brine collection at the air-ice interface.

Single snow particles blown onto a smooth ice sheet were observed (at OB6 to OB11). They acted to enhance the roughness of very new ice by creating an "orange peel" surface, resulting in changes in backscatter intensity at small wavelengths. It was observed that when snow particles are deposited onto new ice that brine is wicked from the ice layer and deposited about the snow particles. The particles melt, diluting the brine solution, and eventually refreeze creating small roughness defects (i.e. mounds). This is illustrated in the series of diagrams presented in Figure 8. Scattering intensity changes due to this small increase in roughness were not observed at 5.3 GHz.

Summary

In summary, it is shown that very new ice undergoes a rapid transition during which the initial ice skim begins with a dielectric constant of sea water and then transforms to a dielectric within a factor twice that of pure ice (3.14). Visual observations suggests that this transition is also associated with a change in the structure of the new ice layer, one with stellar crystals interwoven on the surface to one with a thin bubble-and-brine free surface layer. It is observed that new ice grown

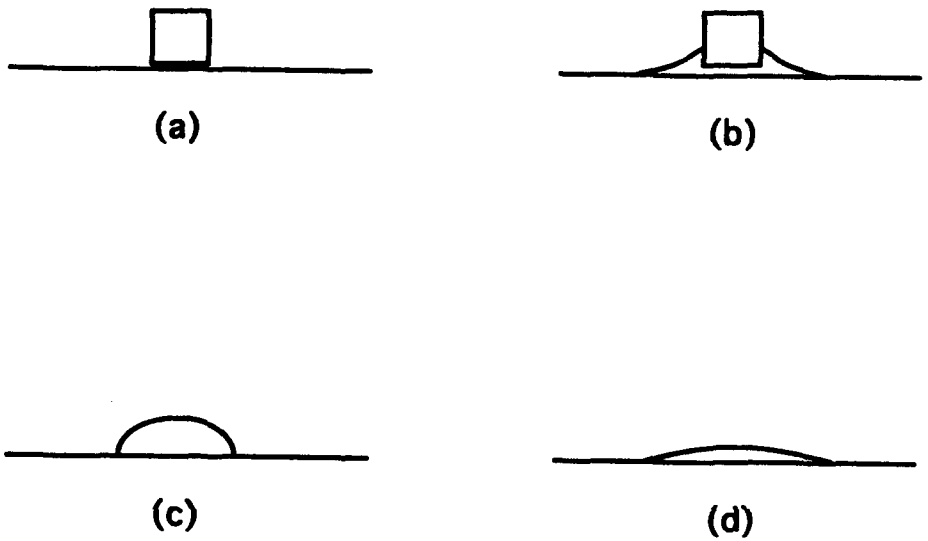

Figure 8. A Naturally Smooth Ice Sheet May Become Roughened When Snow Crystals Are Blown Onto an Ice Sheet. Brine Is Wicked by the Crystals (a), the Crystals May Melt Creating a Diluted Brine Solution (b). A Roughness Defect Will Form on the Surface Upon Freezing of the Brine Solution (c).

under calm conditions has a very smooth ice-air interface. The surface, which is very smooth once the ice skim forms, becomes extremely smooth, and then roughens due to the deposition of single snow crystals. The influence of increased air temperature (from -15° to -5°C) and solar heating on a thin ice sheet is shown to produce an enhanced backscatter at all angles. Additional brine liquid is known to be produced with the elevation of ice temperature. A 7.5 dB reduction in the reflectivity occurs for ice between 0-1 cm and ice of 4-7 cm. The magnitude of this reduction is determined largely by the change in the magnitude of the dielectric constant from 43 to 6 which accounts for a 7.3 dB change in reflectivity.

3.2 TIME SERIES FREQUENCY RESPONSE AT 5 TO 17 GHZ

The relationship between frequency (5 to 17 GHz) and penetration depth for new ice is important; the average dielectric properties of an ice sheet are defined by this depth. The penetration depth is the distance a radio wave propagates before its two-way return value is reduced by 9 dB. It is understood that longer wavelengths penetrate farther into young ice than shorter wavelengths. To illustrate the frequency response of new ice the reflectivity responses at 5.3, 9.6, 13.6, and 16.6 GHz are presented in Figure 9a.

To examine the transition from State 1 to State 2, the average dielectric constant for 0.1 to 2.0 cm thick ice and the minimum value immediately at the beginning of State 2 are used. The associated change in reflectivity is 5, 3, 2, and 2 dB for these four frequencies, respectively. These observations document that the reflectivity and bulk dielectric constant (one more similar to that of sea water and the other more similar to that of pure ice) transition between states occur more quickly and less dramatically at the highest frequencies and are the slowest and most dramatic at the lowest frequencies. Important interrelationship to be highlighted here are between ice surface temperature, salinity, and dielectric constant. At cold

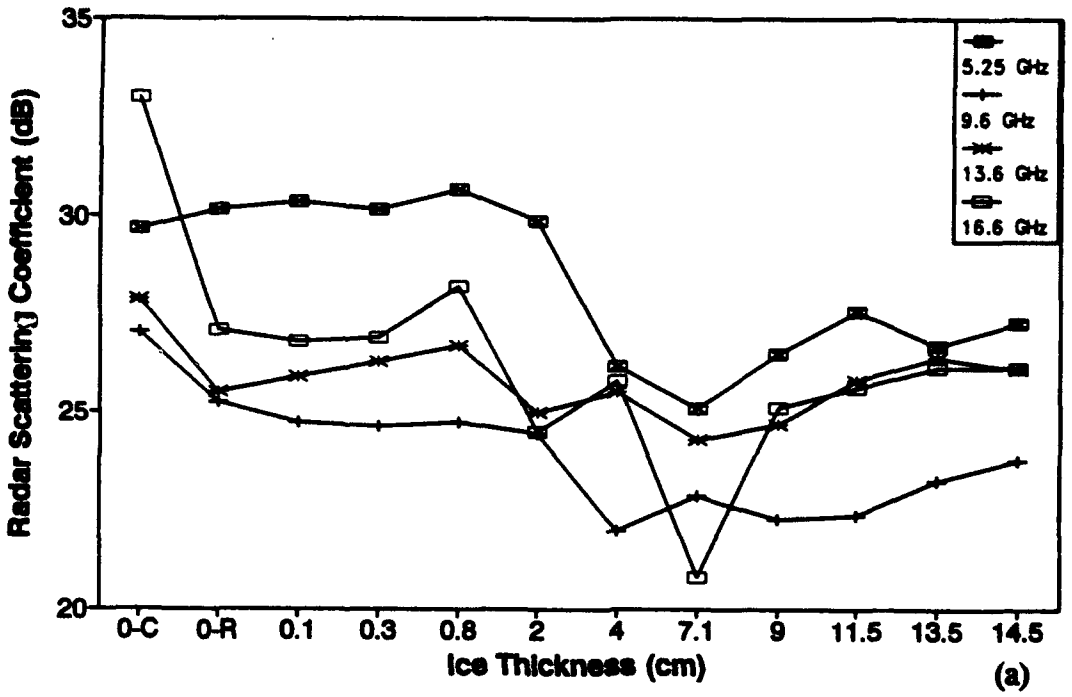

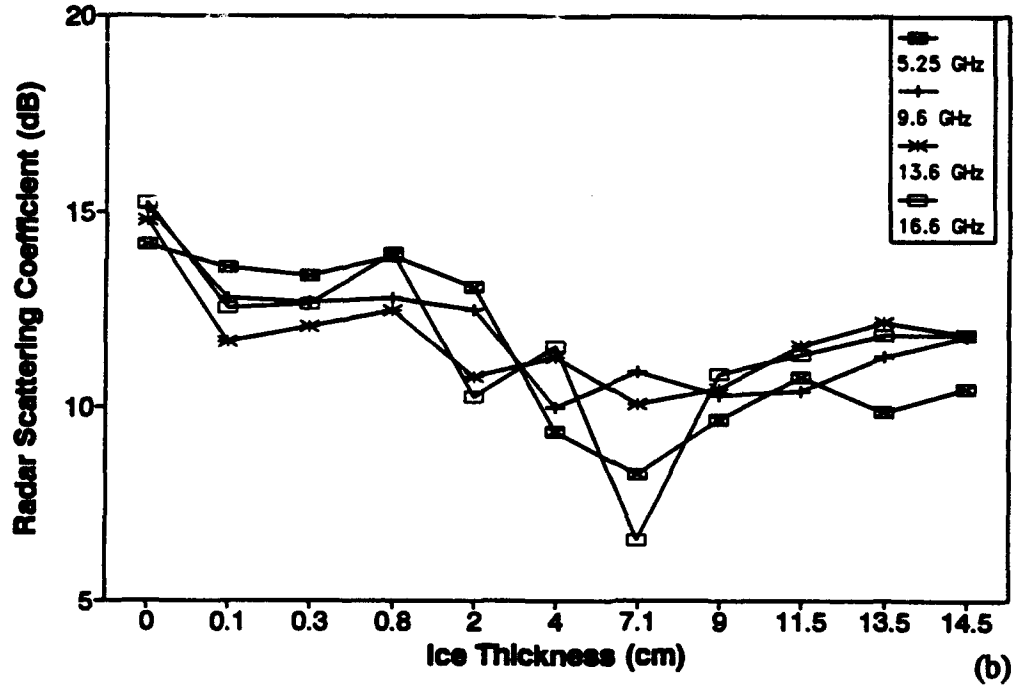

Figure 9. The Time Series Response of Backscatter at Vertical (0°) During the Evolution of Water to Grey Ice Is Shown as a Function of Frequency From 5.3 to 16.6 GHz in (a). Reflectivity Is Normalized by the Square of the Wavelength in (b).

temperatures each of these parameters decrease with increasing ice thickness. Upon correlation of the physical observations (See Figure 3) and the reflectivity response, it is noted that each shows a large change in slope at ice thicknesses between 0.5 and 2 cm. Hence, the changes in reflectivity as related to frequency are associated with processes whereby the upper most portion of the ice sheet transforms more quickly to a lower dielectric constant (i.e., the cooling is top-down), with an interior which lags behind and will always be warmer than the surface.

A modified version of a model developed by Kovacs et al. (1986) is used to predict dielectric profiles so that penetration depths and bulk dielectric constants may be calculated at each of these frequencies. These results are included in Figure 7 and 10 and Tables 3 and 4 for reference and study.

Observations at 9.6 to 16.6 GHz show that very new sea ice attains a dielectric constant much smaller (about 4 times) than that of open water T = 0° immediately upon the initiation of the ice growth process (See Figure 7). Between 0.1 and 0.8 cm, the slope of the reflectivity response increases and the largest change occurs at the highest frequency. In addition, there is a peak at 0.8 cm. These observations argue that brine is expulsed to the surface during the freezing process, that there is a peak in the accumulation (in this study at $\approx$ 1 cm) and that a large percentage change in the dielectric constant occurs in association with the peak in brine accumulation. This brine expulsion event also occurs prior to the transition between State 1 and State 2. Visual observations of this transition document the presence of a thin liquid brine layer during State 1, a peak in visual wetness for ice $\approx$ 1 cm, followed by a sparse distribution of salt crystals on a dry ice surface after the transition to State 2.

A frequency dependency is not seen in association with when the lowest dielectric constant of the ice sheet is attained. This was achieved at 7 cm. However, the ice thickness at which the lowest backscatter cross-sections is observed is frequency dependent. Backscatter nulls are at a thickness of 11 cm for 5.3 GHz, 4

cm for 9.6 GHz, and 2 cm for 13.6 and 16.6 GHz. The magnitude of the backscatter response is driven by the dielectric constant. The effective bulk dielectric constant is determined by penetration depth which is frequency dependent. Furthermore, the C-shape of a salinity profile modulates further the effective dielectric constant, especially at high frequencies, because of the enhancement of the brine volume in the upper most portion of the ice sheet. Examination of the penetration depths provided in Table 3 shows that the backscatter response at 5.3 GHz is influenced by the entire dielectric layer for thicknesses from 0 to 2 cm. In contrast, at 16.6 GHz the top 0.5 cm sets the absolute level of the backscatter response. Recall that the shape function (i.e. the angular response) is largely determined by the surface roughness statistics for new ice and that these properties are relatively constant for thicknesses from 0-5 cm. By the time 4 cm ice is achieved, the bulk dielectric constant magnitudes are essentially independent of frequency (all values are within 5.5% of the mean of 5.1). What is suggested by the above is that 3 penetration depths are required to fully describe the backscatter response and that a dielectric half-space is not achieved until the 3 penetration depth location lies within the ice interior.

Comparison of Normalized Reflectivity Response

The total backscatter may be described as the sum of a coherent and a non-coherent component. The coherent component arises from the backscatter at vertical which originates in association with the specular scattering from a plane. This backscatter σ°_{coh} may be described as

$$\sigma^\circ_{coh} = \pi k^2 |\Gamma^2| \exp(-4\sigma_{surf}^2 k_o^2) \qquad (5)$$

where Γ is the Fresnel reflection coefficient, σ_{surf} is the rms roughness of the air-ice interface, and k_o is the wavenumber in air. Therefore, differences in scattering intensity are proportional to the difference in the dielectric constant and wavelength

Table 3.
Predicted Penetration Depths for Sea Ice With Thicknesses From 1-8 cm.

	PENETRATION DEPTH (cm)			
ICE THICKNESS - cm -	f = 5.25 GHz	f = 9.6 GHz	f = 13.6 GHz	f = 16.6 GHz
1	> 1	0.8	0.5	0.4
2	2.0	1.0	0.7	0.5
4	3.3	1.6	1.0	0.8
8	3.7	1.6	1.0	0.8

squared. A normalization is presented in Figure 9b to remove the wavelength effect. The measured coherent responses track each other closely. The reflectivity at these frequencies is expected to be similar in intensity level once normalized and responses to the changing ice conditions should be similar.

The reflectivity responses are seen to be similar, in general. From 0 to 0.8 cm the reflectivities track within a 1 dB interval. By 2 cm the reflectivity is in transition to a level corresponding to a lower dielectric constant value. Null are attained by 7 cm. Increasing ice thickness beyond 9 cm is also accompanied by increasing air temperature. An air temperature increase from -15° to -10°C results in a 1-2 dB change in reflectivity.

3.3 DIELECTRIC PROPERTIES OF SEA ICE

The complex dielectric constant ϵ_r^* may be represented as

$$\epsilon_r^* = \epsilon_r' - j\epsilon_r'' \tag{6}$$

where ϵ_r' and ϵ_r'' represent the real and imaginary parts. The backscatter response at vertical is proportional to the reflectivity Γ where

$$\Gamma = \left| \frac{\sqrt{\epsilon_r^*} - 1}{\sqrt{\epsilon_r^*} + 1} \right|^2 . \tag{7}$$

3.3.1 Measured Dielectric Properties of Sea Ice

The dielectric constant of sea water has been modeled by Klien and Swift (1977). The dielectric constant and reflectivity Γ_{sw} for sea water at -1.8°C and a salinity of 22 ppt is provided in Table 3. The reflectivity for sea water is then given by

$$\Gamma_{ice} = \Gamma_{sw} * (P_{ice} / P_{sw}) \tag{8}$$

where Γ_{ice} is the reflectivity for the ice sheet floating on sea water, P_{ice} is the power return from the ice sheet, and P_{sw} is the power return from the sea water.

For typical ice conditions $\epsilon_r' > \epsilon_r''$, ϵ_r' will range from 4-10. Based on the magnitude of the reflectivity alone, ϵ_r'' cannot be retrieved. However, $|\epsilon_r^*|$ can be estimated, typically better than 2% for thin and thick ice sheets. The ice reflectivity is related to the complex dielectric constant for ice through

$$\Gamma_{ice} = \left| \frac{\sqrt{\epsilon_{rice}^*} - 1}{\sqrt{\epsilon_{rice}^*} + 1} \right|^2 . \tag{9}$$

The magnitude of the complex dielectric constant may be inverted when Γ_{ice} is measured as is expressed as

$$|\epsilon_{rice}^*| = \left\{ \frac{1 + \Gamma_{ice}^{1/2}}{1 - \Gamma_{ice}^{1/2}} \right\}^2 . \tag{10}$$

If the reflectivity of the open ocean water is calculated based on both ϵ_r^* and $|\epsilon_r^*|$, the reflectivity based on ϵ_r^* is larger by about 2% (0.17 dB). For a case where $\epsilon_r^* = 5\text{-}j1$, the error in reflectivity is about 1%. However, in the case of the inversion on $|\epsilon_r^*|$ for sea water and based on an error free measurement of reflectivity, the implementation of eq(10) results in a poor estimate of the dielectric constant magnitude and is in error by approximately 18%. However, for the case of an ice layer, the error is smaller between 1-2%. Through the utilization of the dielectric property model the relative magnitudes between the real and imaginary parts may be predicted and used to improve the accuracy further. This becomes important when $|\epsilon_r^*|$ is greater than 10.

3.3.2 Dielectric Property Model of Sea Ice

The dielectric model predictions are based on a two-phase dielectric mixing model by Tinga et al. (1973). In addition, the characterization of the complex dielectric constant of pure ice and brine, brine volume, and the effect of the sea ice structure on the orientation of an external electric field relative to the ice structure is required. Formulations which model these parameters and interrelationships between ice density, brine permittivity, temperature profile, and solid salt precipitation are provided by Cox and Weeks (1985), Assur (1960), Tiphane and St.-Pierre (1962), Morey et al. (1984), and Stogryn (1971).

3.3.3 Examination of Measured and Predicted Dielectric Constant

Measured and predicted dielectric constants are presented in Figure 7 and Table 4. Values of dielectric constant were not predicted for ice thicknesses less than 0.8 cm. The most dramatic difference is associated with the measured response at 5.3 GHz and thicknesses less than 0.1-2 cm thick. For frequencies greater than 6 GHz, there is a rapid decrease in dielectric constant magnitude from open water to 0.1 cm thick ice. At 5.3 GHz the change in dielectric constant from open water is gradual. The measured dielectric constants for the various frequencies merge, essentially, by 4 cm. The dielectric constants values at 9-17 GHz are similar and the drop in value from open water to new ice is very rapid, values stay elevated until ice 4 cm thick is attained. In Figure 10 the prediction of the penetration depth for ice thicknesses from 1-8 cm are presented. In the case of 5.3 GHz the penetration depth is greater than or equal to the ice thickness for 1 and 2 cms. A penetration depth which is greater than the ice thickness indicates that the effective dielectric constant is not determined solely by the ice layer, but by both the ice and underlying sea water. Until the penetration depth is less than the ice thickness, the bulk dielectric constant will be greater than those values predicted using the mixing model. After 4 cm,

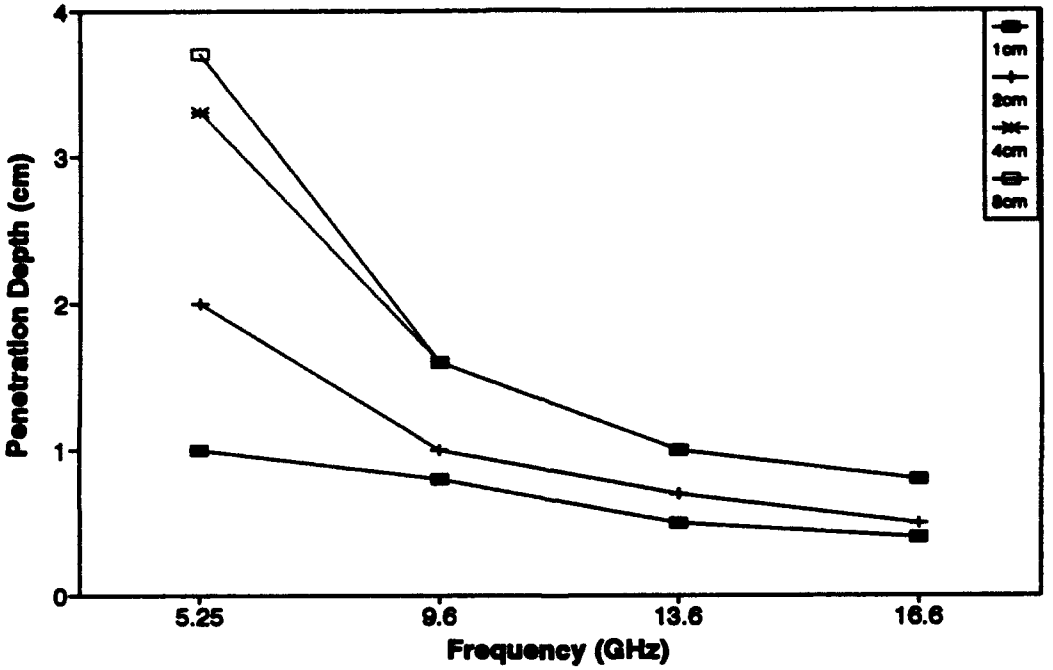

Figure 10. The Penetration Depth Is Shown as a Function of Radar Frequency From 5 to 17 GHz and for Four Ice Thicknesses Which Range From 1 to 8 cm.

Table 4.
Measured and Predicted Dielectric Constant Magnitudes

OBS #	ICE THICKNESS - cm -	MEASURED				PREDICTED			
		5.3 GHz	9.6 GHz	13.6 GHz	16.6 GHz	5.3 GHz	9.6 GHz	13.6 GHz	16.6 GHz
1	0	73	57	46	39	73	57	46	39
2	0.1	43.7	14.9	10.0	10.6	--	--	--	--
3	0.3	37.9	14.3	11.4	11.0	--	--	--	--
4	0.8	55.4	14.8	13.3	18.6	10.1	9.7	8.9	8.7
5	2	31.1	13.2	7.6	5.6	6.8	6.6	6.3	6.0
6	4	7.1	6.2	8.8	7.8	5.3	5.2	5.0	4.8
7	7	5.5	7.8	6.3	3.0	4.2	4.1	4.0	4.0
8	8	7.7	6.6	7.0	6.5	4.0	3.9	3.9	3.8
9	11	10.8	6.8	9.7	7.4	6.2	5.9	5.8	5.6
10	13.5	8.2	8.7	11.8	8.5	4.6	4.5	4.4	4.3
11	14.5	9.8	10.2	10.7	8.5	4.3	4.2	4.1	4.0

predicted and measured dielectric constants begin to track each other, except measured values are twice those predicted based on 1 penetration depth. When air temperatures increase, the measured dielectric constant trend increases greater than that indicated by just the warming of the ice sheet. This suggests that the influence of the development of a thin wetness layer which coats the ice surface must be accounted for.

3.4 MEASURED AIR AND ICE TEMPERATURE RELATIONSHIP

Air and surface temperatures were measured during the evolution of sea ice from open water to 15 cm ice. During the first 31 hours, ice grew to a thickness of 8 cm. Air temperature at the time of measurement was reasonably constant at about -15°C. After 31 hours air temperatures increased to about -10°C. In Figure 11 ice surface temperatures are shown as a function of thickness for these two air temperatures. The relationships between T_{air}, T_{ice}, and ice thickness is examined for these two air temperatures separated by about 5°C and ice thicknesses from 2-21 cm were found to be

$$T_{ice} = -3.9 + \delta_{ice}*(-0.032) \text{ for } T_{air} = -9.9 \pm 0.8°C \text{ and } \delta_{ice} = 5\text{-}21 \text{ cm} \quad (11)$$

$$T_{ice} = -4.7 + \delta_{ice}*(-0.307) \text{ for } T_{air} = -15.4 \pm 0.3°C \text{ and } \delta_{ice} = 2\text{-}19 \text{ cm}. \quad (12)$$

For the cases of $T_{air} \approx -10°C$, the ice temperature was reasonably constant (slope = -0.032°C/cm) for ice thickness from 5-21 cm at a temperature of -4.25°C ±0.17°. For the case of cooler temperatures at about $T_{air} \approx -15°C$, the ice temperatures are found to have a strong relationship with T_{air} for ice thicknesses from 2-19 cm, the slope is -0.31°C/cm. The correlations for the above relationships are 0.59 and 0.75, respectively.

Results in this report document how changes in T_{air} impact backscatter intensity and the modification of the bulk dielectric constant. When the ice surface temperatures are in the region of -4°C, the change in permittivity is much greater than when temperatures are < -8°C.

In the region near a thickness of 2 cm, ice sheet temperatures are within 1°C. As ice thickness increases beyond 2 cm, ice surface temperatures (for $T_{air} = -15°C$) decrease rapidly. By an ice thickness of 20 cm, the temperature difference has

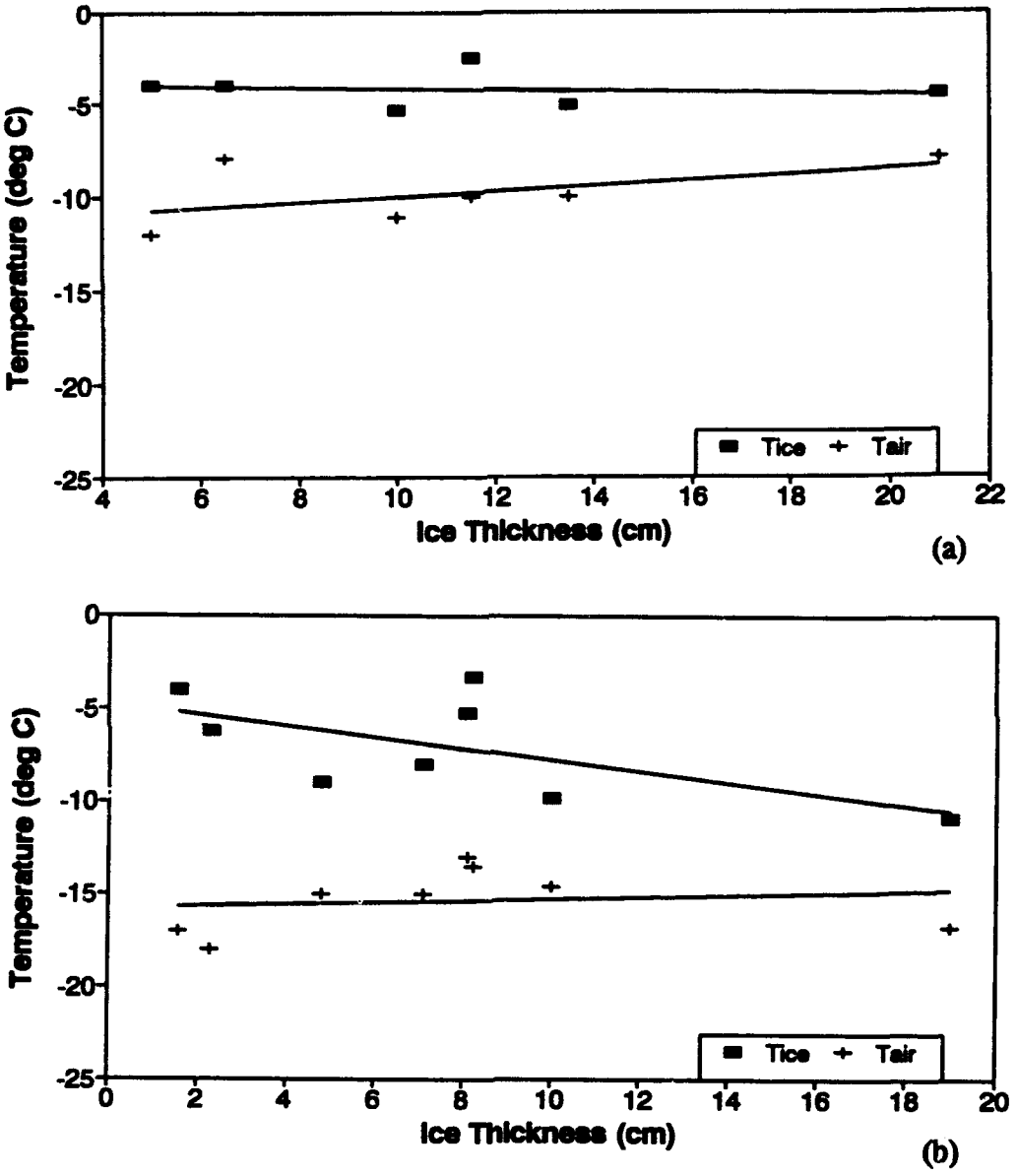

Figure 11. The Relationship Between Air Temperature, Ice Temperature, and Ice Thickness Is Shown in (a) for an Air Temperature of About -10°C, in (b) for an Air Temperature of About -15°C. For the Warm Temperatures, There Is Little Variation With Ice Thickness (T_{ice} = -4.25 ± 0.2°C). For Cold Ice, There Is a 0.31°C/cm Decrease With Increasing Ice Thickness.

reduced from 13° to 6°C.

3.5 BACKSCATTER RESPONSE DURING THE GROWTH PHASE

Discussed in the following sections are the backscatter responses for 5.3, 9.6, 13.6, and 16.6 GHz. Effects due to solar influences and brine expulsion are highlighted and discussed.

3.5.1 Backscatter Response at 5.3 GHz

In the transition for water to grease ice (δ_{ice} = 0.1 cm), little change is noted in reflectivity levels. This argues that the open water surface is smooth (it was) and the ice layer is thin compared to the radar wavelength (it was). Backscatter of ice in the thickness region from 0.1-9 cm shows a continuous reduction in intensity. The backscatter response is observed to decay beyond that predicted by the change in reflectivity. Based on this result, it is hypothesized that the ice-bottom/sea-water interface is contributing to the microwave response. As is indicated by the value of the penetration depth, the radar signal may originate beyond the ice-water interface. At this wavelength, backscatter is attributed largely to scattering from interfaces. Volume scatter for new and thin ice has been shown by Kim et al. (1984a) to be small due to a lack of discrete scatterers within an order of magnitude of the wavelength in ice . For these ice cases the brine pocket represents the most probable discrete scatter source, but with radii of 0.025 mm, they are about 700 times smaller than the radar wavelength in ice ($\lambda_{ice} = \lambda_{air}(\epsilon_r')^{-2} \approx$ 1.8-2.3 cm).

In the transition from State A to State B, the backscatter intensity at angles from 25° to 40° and VV-polarization reduces about 16 dB. An important issue is how to account for this reduction. A change in 4.8 dB may be attributed to the change in reflectivity from State A to State B. An additional decrease of 4.5 dB may be attributed to a reduction in surface roughness (e.g. the change from stellar crystals to a very smooth surface). To account for the final 7 dB requires the contribution of

a three layer dielectric system with plane boundaries. This will be investigated in future work to study the frequency and angular responses. A model has been developed which will allow study of these effects [personal communication, Adrian Fung, 1992]. This will be the subject of a future analysis.

Solar Effects

The divergence in the backscatter response at 9 and 11 cm is attributable to the 5°C warming of the ambient air temperature as is indicated by the increase in reflectivity (1.1 dB). A divergence in the VV and HH responses is expected if there is an increase in the effective dielectric constant this is observed.

The enhancement in association with the transition from ice 11 to 13.5 cm thick is significant (7.8 dB) It also occurs with a slight reduction in the reflectivity. The environmental conditions show a 2.6°C reduction in ice surface temperature during this 20 hour period. Observations of the 11 cm thick ice were conducted when it was sunny, whereas the 13.5 cm ice observations were made during late morning without sun. Given the observed angular response it is hypothesized that the warming-cooling process has in effect produced an internal dielectric roughness. The cooling of the ice surface temperature is accompanied by a slight reduction in reflectivity, hence, an accompanying reduction in bulk dielectric constant. The enhancement of the backscatter at 25° and 40° was not caused by an increase in the roughness of the air-ice interface; no significant change was observed. An ice sheet which does not cool uniformly in the vertical dimension of the ice sheet has the potential to create a rough dielectric structure, and enhance the radar backscatter. This structure was not anticipated and, therefore, was not monitored. Future observations will be needed to account for this possibility.

The slight reduction in the backscatter response from 13.5-14.5 cm thick ice is expected, based upon the above, due to additional cooling in the 25 hour period.

Note, however, that the backscatter levels observed for 9 cm ice is not expected due to a 5°C higher ice surface temperature.

Brine Expulsion Events

Active microwave observation of the expulsion of brine onto an ice surface is documented and is found to have occurred at ice of 0.8 cm thick. An increase is noted in the reflectivity and measured bulk dielectric constant. Modification of the backscatter response at 25° and 40° and VV and HH polarizations is probably not detectable, except at 16.6 GHz. It is, however, important to note that the transition from State A to State B occurs immediately after this event.

In Figure 12 is a set of four diagrams which illustrate the modes that may occur in association with brine, brine pockets, and expulsion. When brine begins freezing a brine pocket may contain brine and gas (a). With further cooling the brine is concentrated further and additional pure ice is produced (b). Upon further cooling, the brine pocket reduces in size and gas in the pocket compresses further (c). A point is reached when further cooling produces a brine enclosure which can no longer support the forces required to contain the liquid and gas. A failure in the ice column on the microscopic level, probably associated with the ice grain boundaries occurs and allows brine to flow to ice surface in greater abundance than normally present. This process has been described by Bennington (1963) and Untersteiner (1968). The increased wetness is short lived. It is observed that the brine expulsion is accompanied by a visually wetter looking surface. After the transition to State B the top millimeter was observed to become very smooth and translucent.

3.5.2 Backscatter Response at 9.6 GHz

In the transition from open water to grease ice, there is a slight reduction in reflectivity. The reflectivity in the State A region (δ_{ice} = 0.1-2 cm) is stable and

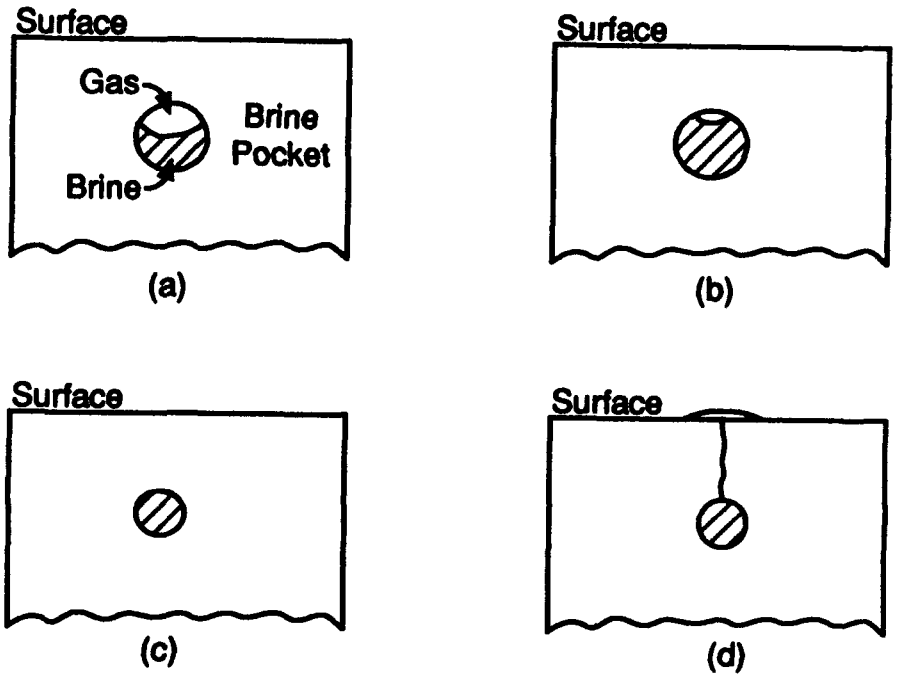

Figure 12. During the Cooling of an Ice Sheet the Properties of a Brine Pocket May Change. In (a) the Pocket Is Shown Containing Gas and Brine, in (b) With Cooling the Pocket May Reduce in Size, in (c) Upon Further Cooling the Pocket May Reduce Further to Its Maximum Diameter, and in (d) Further Cooling Induces a Failure Allowing Very High Salinity Brine to Flow to the Ice Surface.

changes little, except when it transforms to State B (a null is attained at 4 cm). The reflectivity in the State B region varies little. The backscatter at VV for angle of 25° and 40° show a steady reduction in backscatter from that observed for open water until about 2 to 4 cm, depending on the angle (See Figure 13). Backscatter increases to about 9 cm. The response for HH polarization is found to increase from 0.8-9 cm. Whether the backscatter response for the transition from open water to 0.8 cm decreases or increases is found to depend on the incidence angle. The State B response is attained by 4 cm. It is accompanied by an increase in backscatter intensity at both VV and HH polarizations. Reflectivity is reasonably constant. It is anticipated that both volume and surface scattering may increase with increasing ice thickness due to a colder ice sheet, the desalination of the upper ice sheet, and the increase in porosity of ice near the air-ice interface. Observations of the physical properties do not necessarily explain the increase in intensity seen at 9 cm. Backscatter levels are the same as those observed for the open water, except at HH-40°. The backscatter response at VV and HH merge at 7 cm.

Solar Effects

Changes in the backscatter response at this frequency is also observed for ice from 9-14.5 cm thick and are associated with changes in ambient air temperature and solar effects (bright sun on ice sheet or no sun). The observation of 9 cm ice represents the cold ice case. Observations which follow are associated with heating and cooling of the ice sheet. With the increase of the T_{ice} from -10° to -2.5°C, the backscatter intensity at 25° and 40° decreases several dB at both VV and HH polarization. The reduction in backscatter is the least at VV-25°, about 2 dB. This may be important in that it suggests that the ice appears smoother (reductions at angles less than about 25° are most sensitive to surface effects), whereas the decrease in backscatter at the large angles is an indication that volume scattering may be

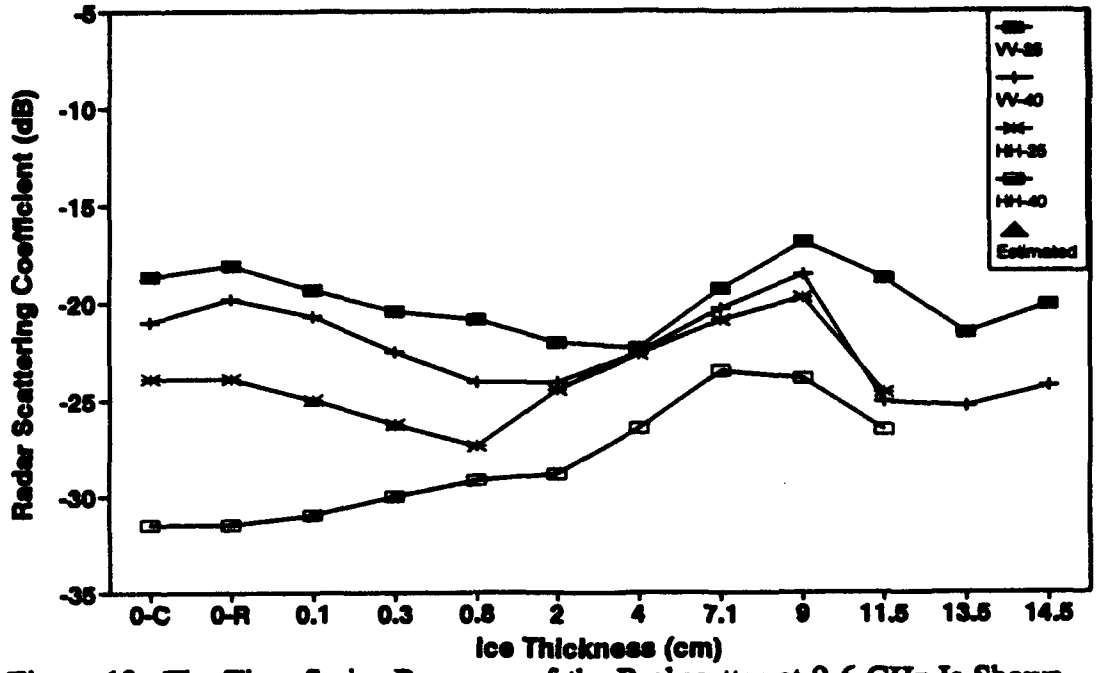

Figure 13. The Time Series Response of the Backscatter at 9.6 GHz Is Shown for the Evolution of Open Water to Young Ice at Incidence Angles of 0°, 25° and 40° for VV and HH Antenna Transmit-Receiver Polarizations.

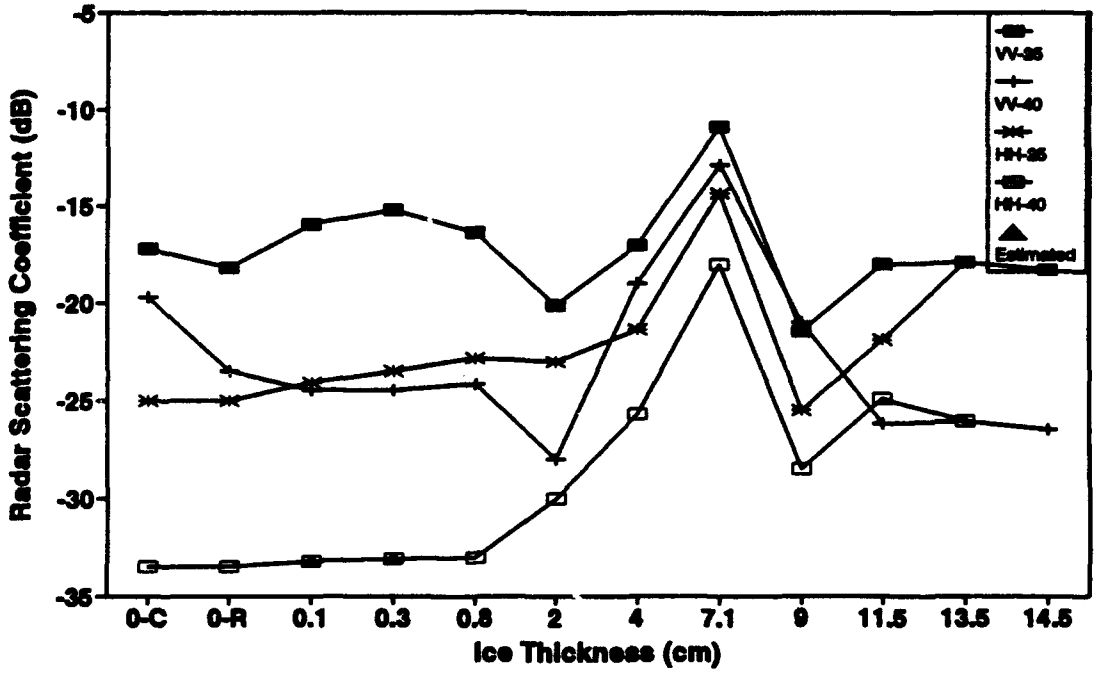

Figure 14. The Time Series Response of the Backscatter at 13.6 GHz Is Shown for the Evolution of Open Water to Young Ice at Incidence Angles of 0°, 25° and 40° for VV and HH Antenna Transmit-Receiver Polarizations.

reduced due to an elevated dielectric constant. This volume scattering reduction is greater than that which may be attributed to a change in surface roughness, no significant change in surface roughness is noted. The surface was smooth for the 9-11 cm thick ice. The change from 11-13.5 cm thick ice is in association with a reduction in T_{ice} of about 2.5°C. The increase in reflectivity argues that the bulk of the ice sheet has warmed even though the ice surface is cooling. The backscatter intensity either stays the same (VV-40°) or reduces further (VV-25°) depending on incidence angle. The effects of warming may have further smoothed an already very smooth surface by an action of superficial surface melting and refreezing (as suggested by the response at VV-25°). The transition from 13.5-14.5 cm thick ice represents further cooling of the ice sheet for an additional 25 hour period. This additional cooling time does not change the T_{ice} but allows the temperature profile in the ice interior to become more linear, i.e. the interior ice is cooler. However, a very thin wet surface layer has formed due to the presence of the sun and the backscatter intensity is seen to increase at both 25° and 40°. This increase is explained by the increase in reflectivity. The methodology to measure *in situ* thin layers had not been developed at the time of this investigation.

3.5.3 Backscatter Response at 13.6 GHz

One of the key features of the backscatter response at this frequency is the steady increase in reflectivity and backscatter at VV-25° from 0.1-0.8 cm (See Figure 14). This suggest that the build up of the brine layer is occurring during this entire transition. Peak brine layer effect is seen at a thickness of 0.8 cm and the transition to State B occurs immediately thereafter. The responses at 25° and 40° for either VV or HH polarizations are different than those observed at either 5.3 or 9.6 GHz.

The transition of open water to grease ice suggests a surface which has transitioned from rough to smooth. The backscatter at VV-25° shows an

enhancement while the backscatter at VV-40° shows a reduction. This suggests a change in both that the correlation length and rms height. The transition from State A to State B occurs from 0.8-2 cm. The backscatter response at HH-polarization increases, as is the case for 9.6 GHz. The reflectivity for State B is stable, and the backscatter at VV and HH polarizations increase from 2-9 cm. A peak in backscatter is seen for 7 cm thick ice. The increase in backscatter from 2-7 cm is attributed to increases in volume scattering in association with changes in the upper ice sheet and the introduction of 1 cm of natural snow. The largest increase in backscatter (about 12 dB) is seen at 40° at HH polarization. The reduction from 7 and 9 cm thick ice is attributed to the removal of the thin snow layer.

The response from 9-14.5 cm ice is similar to that observed at 9.6 GHz. The reduction in volume scatter due to a warming ice sheet is the process which dominants.

3.5.4 Backscatter Response at 16.6 GHz

The wavelength at this frequency is more than 3 times smaller than the wavelength of the lowest frequency in this study. Reaction to small changes in the ice sheet is also expected to be the greatest. This frequency shows its largest change in reflectivity when transitioning from water to grease ice (See Figure 15). The reflectivity in the State A region decreases slightly with increasing ice thickness, except for an enhancement associated with brine expulsion at 0.8 cm. Importantly, the change in reflectivity due to this event is the greatest at this frequency. The response to the brine expulsion event is also apparent in its effect on VV-25° and results in an increase in backscatter intensity.

Significant enhancement in backscatter also occurs at 4 cm. Why this occurs cannot be explained at this time. However, the trend from 9 to 13.6 GHz when extrapolated to 16 GHz an enhancement may occur. The greatest backscatter

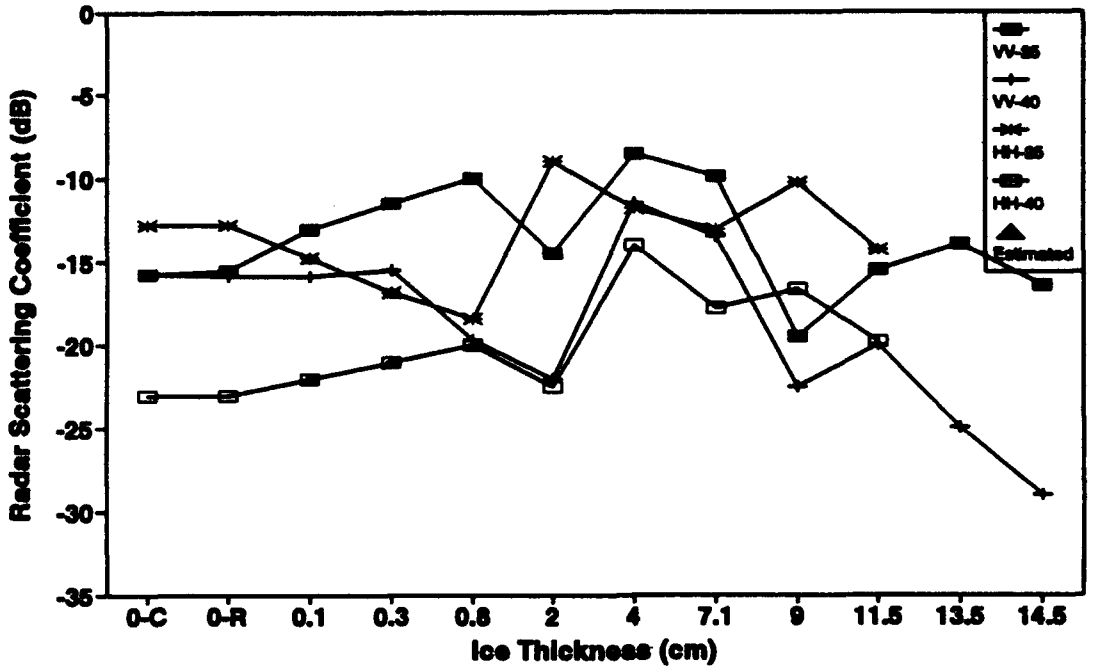

Figure 15. The Time Series Response of the Backscatter at 16.6 GHz Is Shown for the Evolution of Open Water to Young Ice at Incidence Angles of 0°, 25° and 40° for VV and HH Antenna Transmit-Receiver Polarizations.

enhancement may also be expected to occur at 40° in association with the addition of volume scattering due to the snow layer. This did not occur, but intensity levels are already very high. The transition from 4 to 7 cm results in a slight reduction and suggests that the snow layer is interfering with the effect which dominated the 4 cm response.

The study series from 9-14.5 cm thick ice shows a similar trend to that observed at 13.6 GHz, but the reduction in backscatter at 40° is even more dramatic. This reinforces the hypothesis that is presented earlier. The production of volume scattering is expected to be the greatest at the highest frequency. The response at this frequency to elevated ice sheet temperatures and the production of a free water layer on the ice surface is also expected to be the greatest. The effect of solar heating by the sun is observed to be the most dramatic at the highest frequency used in this study.

3.6 POLARIZATION RATIO RESPONSE DURING THE GROWTH PHASE

The backscatter at VV and HH polarization change in response to the dielectric constant profile of the ice sheet and surface roughness. The ratio of the these two polarizations is of interest because it affords an additional means to examine how a target response changes with incidence angle, frequency or environmental conditions. The polarization ratio *PR* is defined here as

$$PR = \sigma^{\circ}_{VV} / \sigma^{\circ}_{HH} . \qquad (13)$$

Since $\sigma^{\circ}_{VV} > \sigma^{\circ}_{HH}$ typically, this ratio is greater than 1 or positive when expressed in decibels. Simulations and measurements by Onstott et al. (1991) suggest the following rules of thumb:

(1) Polarization ratios are the greatest for large dielectric constants (e.g. those of sea water) and smooth surfaces,

(2) Polarization ratios increase with increasing incidence angle and is 1 at 0°.

(3) Polarization ratios become small when the dielectric constant of first year ice is attained or when the surface becomes very rough ($\sigma_{surf} \geq 0.5$ cm rms).

The ice thickness for which the maximum of the polarization ratio is observed is found to be a function of frequency as seen in Figure 16. For 5.3 and 9.6 GHz this occurs at a thickness near 0 cm and then increases with increasing thickness. The minimum ratio occurs at ice thicknesses from 2-9 cm. The general trend of the polarization ratio is a gradual reduction with increasing ice thickness. The trend at 16.6 GHz is the most different. The ratio is flat from 0 to about 4 cm at which there is a reversal in both the 25° and 40° responses.

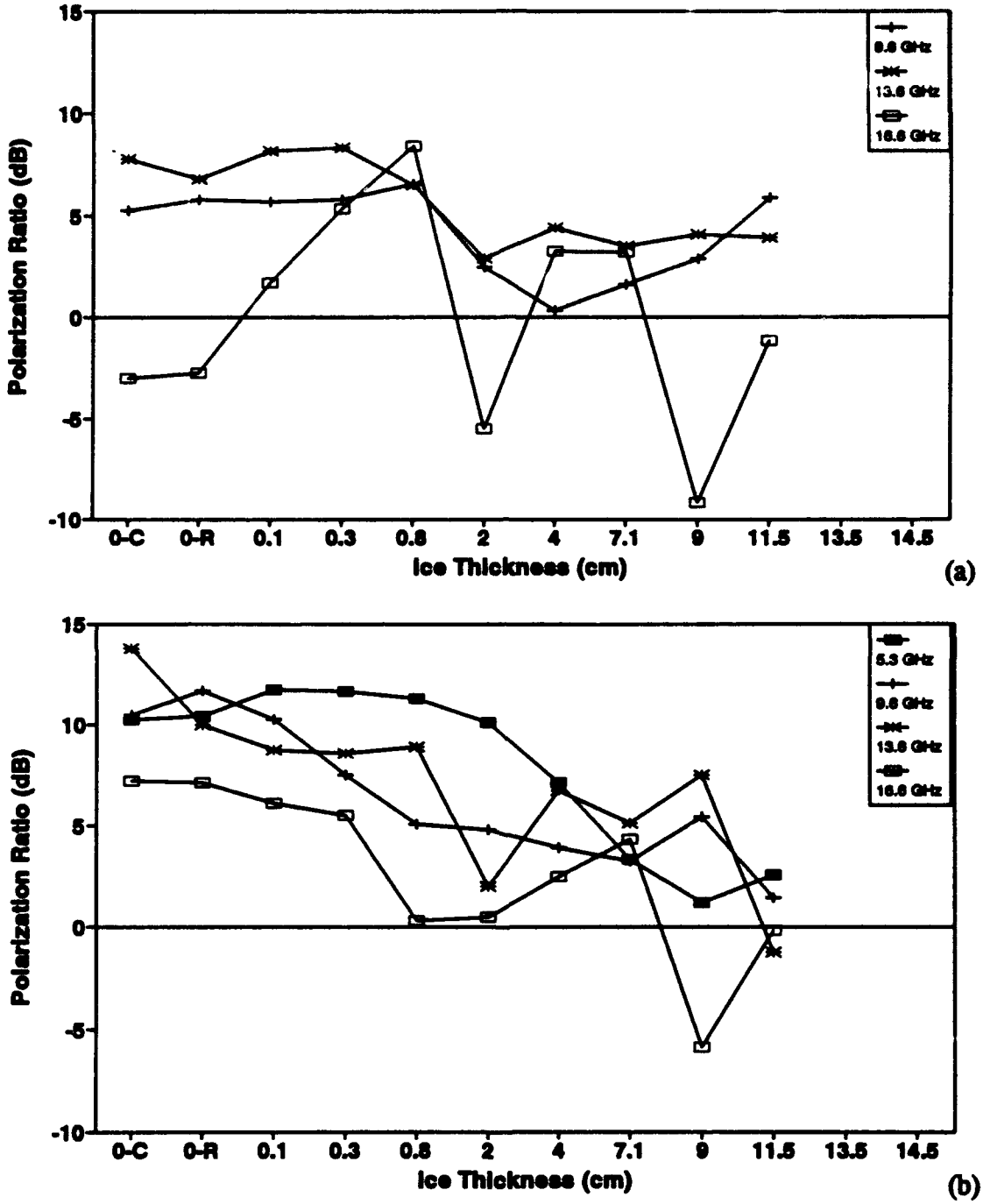

Figure 16. The Polarization Ratio Is Shown as a Function of Ice Thickness and Incidence Angle at 25° and 40° and for Frequencies of 5.3, 9.6, 13.6, and 16.6 GHz.

4.0 SUMMARY

The evolution of backscatter and reflectivity for frequencies from 5-17 GHz is examined for ice thicknesses from 0-15 cm. During the first thirty hours the air temperature is stable and cold ($T_{air} \approx -15°C$) and an ice thickness of 9 cm is attained. Eight observations were made during this period. The microwave signatures of ice of this thickness are expected to be stable, if the ice surface roughness is not changed, snow is not added, and the temperature conditions do not change. During this investigation there are three additional cases examined where an ice sheet experiences several degrees of warming and then cooling within a 46 hour period. Five additional centimeters of ice are also added.

Three dielectric constant states are noted: a scene characterized by a high dielectric constant, one similar to that of sea water; a state in transition; and a low dielectric constant (2-3 times that of pure ice). The expulsion of brine to the ice surface is noted (visibly and through the microwave signature) prior to the transition to the low dielectric state. The association of when the transition begins and ice thickness is found to be frequency sensitive (See Figure 17). The lower the frequency the thicker the ice is before a change in its reflectivity is observed. The general trend for $\sigma°_{VV}$ and $\sigma°_{HH}$ is documented and found to be both a function of frequency and angle. For the 25° angle, the responses when normalized to 5.3 GHz are seen to increase with increasing thickness. In addition, the magnitude of this increase increases with increasing frequency. The 5.3 GHz response is very well behaved and shows a gradual decay to 9 cm. The 5.3 and 9.6 GHz responses are similar from 0-2 cm. At 40°, the normalized responses are similar from 0-0.3 cm and then diverge. The divergence from the 5.3 GHz response is the greatest for the thickest ice and the highest frequency.

The polarization ratio is found to be the greatest for 0-1 cm ice. It then gradually reduces with increasing ice thickness. Each frequency produced its

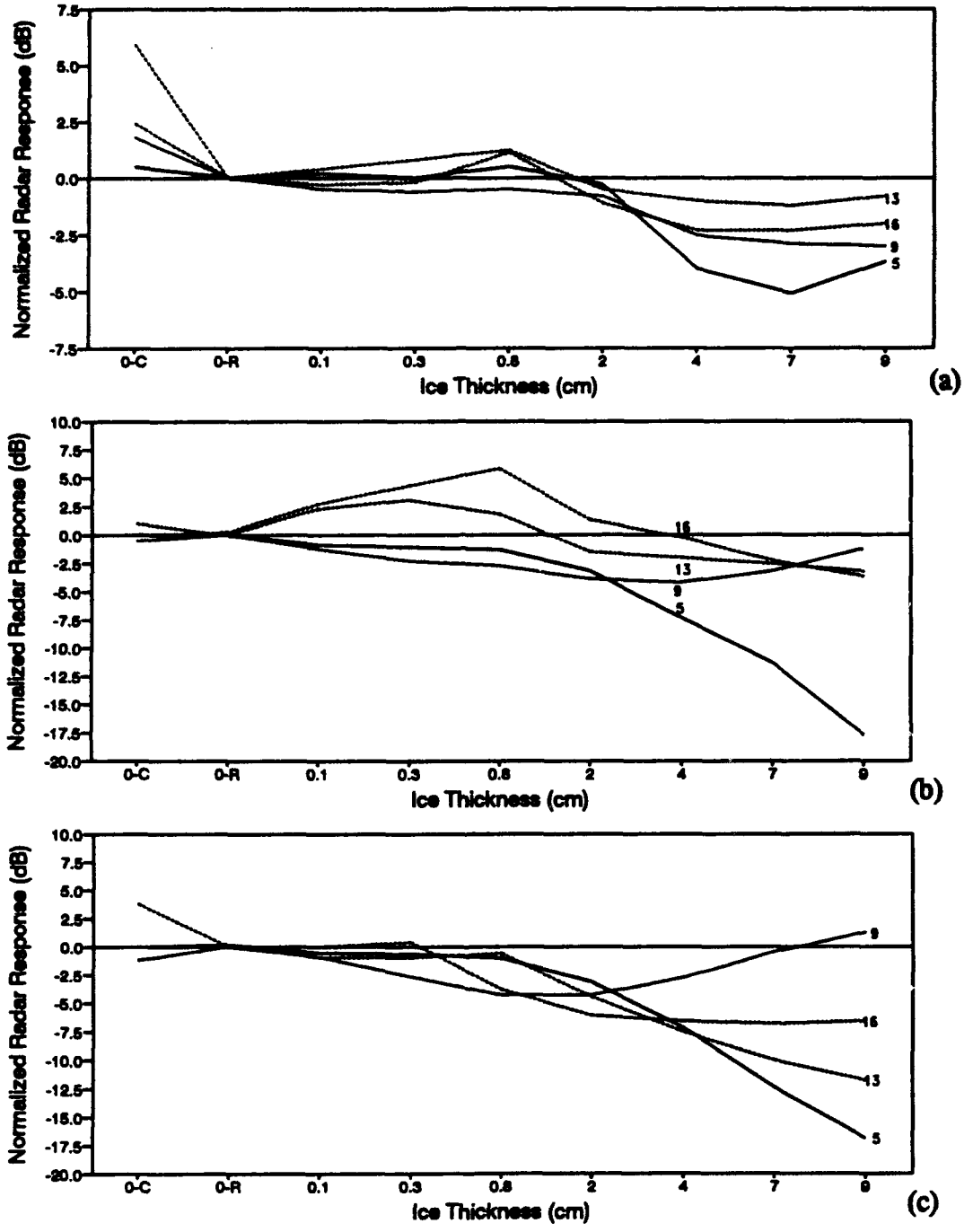

Figure 17. Normalized Radar Scattering Coefficient Response Is Presented to Illustrate the Backscatter Response at Frequencies From 5 to 16 GHz for Various Thicknesses From 0 to 9 cm. The Label 0-R Indicates Open Water With a Rippled Surface, 0-C Indicates That the Water Surface Is Free of Ripples and Winds Are Calm. The Incidence Angle in (a) Is 0°, (b) Is 25°, and (c) Is 40°. The Polarization Is VV.

maximum ratio at different ice thicknesses. The ratio for 16 GHz occurred at the thickest ice of 0.08 cm and was attributed to its sensitivity to the expulsion of brine to the ice surface. The minimum ratios were observed after the transition to the lower dielectric constants. This occurred by a thickness of 11 cm.

REFERENCES

Arcone, S.A., A.J. Gow, and S. McGrew, "Microwave Dielectric, Structural, and Salinity Properties of Simulated Sea Ice," *IEEE Trans. on Geoscience and Remote Sensing*, Vol. GE-24, No. 6., pp. 832-839, November 1986.

Assur, A., "Composition of Sea Ice and Its Tensile Strength," Report No. 44, U.S. Army Cold Regions Research and Engineering Laboratory, Hanover, NH, 1960.

Bennington, K.O., "Some Crystal Growth Features of Sea Ice," *Journal of Glaciology*, Vol. 4, No. 36, pp. 669-688, 1963.

Carsey, F., Editor, *Microwave Remote Sensing of Sea Ice*, American Geophysical Union, Washington, DC, 1992.

Cox, G.F.N. and W.F. Weeks, "On the Profile Properties of Undeformed First Year Sea Ice," U.S. Army Cold Regions Research and Engineering Laboratory, Unpublished Report, 1985.

Gow, A.J., "Orientation Textures in Ice Sheets of Quietly Frozen Lakes," *Journal of Crystal Growth*, Vol. 74, pp. 247-258, 1986.

Kim, Y. S., R. K. Moore, and R. G. Onstott, "Theoretical and Experimental Study of Radar Backscatter From Ice," Report No. 331-37, University of Kansas Remote Sensing Lab, Lawrence, pp. 331-337, January 1984.

Kim, Y. S., R. G. Onstott, and R. K. Moore, "Effect of Snow Cover on Microwave Backscatter From Sea Ice," *IEEE J. Oceanic Eng.*, Vol. OE-9, No. 5, pp. 383-388, 1984.

Kim, Y. S., *Theoretical and Experimental Study of Radar Backscatter From Sea Ice*, Ph.D. Dissertation, University of Kansas, Lawrence, 1984.

Klein, L.A., and C.T. Swift, "An Improved Model for the Dielectric Constant of Sea Water at Microwave Frequencies," *IEEE Trans. Ant. Prop.*, Vol. AP-25, No. 1, pp. 104-111, 1977.

Kovac, A., R.M. Morey, G.F.N. Cox, N.C. Valleau, "Modeling the Electromagnetic Property Trends in Sea Ice and Example Impulse Radar and Frequency-Domain Electromagnetic Ice Thickness Sounding Results," report, U.S. Army Cold Regions Research and Engineering Laboratory, Hanover, NH, July 1986.

REFERENCES (CONTINUED)

Onstott, R.G., "SAR and Scatterometer Signatures of Sea Ice," *Microwave Remote Sensing of Sea Ice*, ed. F. Carsey, American Geophysical Union, Washington, DC, Chap. 5, 1992.

Onstott, R.G., "Examination of the Physical, Electrical, and Microwave Evolution Of Water Into Young Sea Ice." In *Proc. of IGARSS'92*, Clear Lake, Tx, May 1992.

Onstott, R.G., R. Shuchman, and C. Wackerman, "Polarimetric Radar Measurements of Arctic Sea Ice During the Coordinated Eastern Arctic Experiment." In *Proc. of IGARSS'92*, Espoo, Finland, June 1991.

Onstott, R.G., "Polarimetric Radar Measurements of Artificial Sea Ice During CRRELEX '88," ERIM Report No. 196100-23-T, Environmental Research Institute of Michigan, Ann Arbor, April 1990.

Onstott, R.G., D. Xue, and R.K. Moore, "Laboratory-Based Experiment to Study the Active Microwave Response of Artificially Grown Sea Ice," Report No. 314-4, Remote Sensing Laboratory, University of Kansas, pp. 135, August 1985.

Stogryn, A., "Equations for Calculating the Dielectric Constant of Saline Water," *IEEE Trans. Microwave Theory*, Vol. 19, No. 8, pp. 733-736, 1971.

Tinga, W.R., W.A.G. Voss, and D.F. Blossey, "Generalized Approach to Multiphase Dielectric Mixture Theory," *J. Applied Physics*, Vol. 44, No. 9, pp. 3897-3902, 1973.

Tiphane, M. and J. St-Pierre, "Tables de determination de la salinite de l'eau de mer par conductivite electrique," Internal Report, Department of Science, University of Montreal, 1962.

Ulaby, F. T., R. K. Moore, and A. K. Fung, "*Microwave Remote Sensing Active and Passive*," Vol. 2, Addison-Wesley, Reading, MA, 1982.

Untersteiner, N., "Natural Desalination and Equilibrium Salinity Profile of Old Sea Ice." In *The Physics of Snow and Ice: International Conference on Low Temperature Science*, Vol. 1, ed. H. Oura, Sapporo: Institute of Low Temperature Science, Hokkaido University, pp. 569-577, 1967.

REFERENCES (CONCLUDED)

Weeks, W.F. and A.J. Gow, "Crystal Alignment in the Fast Ice of Arctic Alaska," Report No. 79-22, U.S. Army Cold Regions Research and Engineering Laboratory, 1979.

Weeks, W.F. and S.F. Ackley, "The Growth, Structure, and Properties of Sea Ice," Monograph 82-1, U.S. Army Cold Regions Research and Engineering Laboratory, 1982.